2014

Bio-Inspired and Low-Content Polymer Cement Mortar for Structural Rehabilitation

Nima Zohhadi
University of South Carolina - Columbia

BIO-INSPIRED AND LOW-CONTENT POLYMER CEMENT MORTAR FOR STRUCTURAL REHABILITATION

by

Nima Zohhadi

Bachelor of Science
University of Tehran, 2010

Submitted in Partial Fulfillment of the Requirements

For the Degree of Master of Science in

Civil Engineering

College of Engineering and Computing

University of South Carolina

2013

Accepted by:

Fabio Matta, Director of Thesis

Navid B. Saleh, Reader

Paul Ziehl, Reader

Lacy Ford, Vice Provost and Dean of Graduate Studies

DEDICATION

To my parents, for their endless love, support, and encouragement, for my friend for her invaluable friendship, and to my professor at U. SC and all my friends

ACKNOWLEDGMENTS

I would like to express my deepest appreciation to my advisor Dr. Fabio Matta for his guidance, patience and support. Thank you for forcing me to look at research and my work in different ways. Your support was essential to my success here.

I would like to thank my committee members, Dr. Paul Ziehl and Dr. Navid Saleh for their invaluable advice and help throughout my research. My gratitude also extends to my friend and coworker Nirupam Aich. Much of my experimental work would have not been completed without your assistance.

I owe my deepest gratitude to my parents, for their endless love, support, and encouragement. No words can describe my love to you both.

I would like to thank my dearest friend Samaneh Kamali for her invaluable friendship and support in difficult times and my fellow graduate students for their friendship and assistance. I will always remember the great times we had.

At last, I would like to thank the members of my department, Civil and Environmental Engineering Department. The faculty, staff, and students made my stay in Columbia a great experience.

ABSTRACT

The use of polymers as partial replacements for ordinary Portland cement in cement mortar can offset several drawbacks by increasing the tensile strength and ultimate strain, enhancing adhesion to concrete substrates in structural rehabilitation applications, and reducing the permeability. Various polymers with a wide range of physical and mechanical properties have been used in the fabrication of cement composites ranging from mortar to concrete. The typical polymer/cement (p/c) weight ratio for such composites is 5% to 20%. Relevant drawbacks associated with the use of polymer-modified mortars (PMMs) are exacerbated at higher p/c ratios, such as: high cost; vulnerability to high temperatures, chemical attack, and UV radiation; and storage and handling issues such as odor, toxicity, flammability, and combustibility. Finding ways to offset these drawbacks while capitalizing on the advantages offered by PMMs is of significance in the context of infrastructure maintenance and sustainability.

In this thesis poly(dopamine) (PDA) is introduced as a polymeric binder for high-performance PMMs containing small p/c ratios in the range 0.1-0.5 wt%, i.e., one order of magnitude smaller than those used in common PMM mixtures. The formation and microstructure of the PDA-cement matrix is examined at varying p/c ratios. The 7-day and 28-day compressive strength and splitting

tensile strength of prototype PDA-cement mortars were characterized at different p/c ratios. The morphology and microstructure of the PDA-cement matrix were studied using scanning electron microscopy (SEM) and energy-dispersive X-ray spectroscopy (EDX) analysis of samples obtained from fracture surfaces. The effect of PDA on the restrained shrinkage of mortar was also experimentally studied. The incorporation of PDA at a p/c ratio of 0.5 wt% improved the cube compressive strength, splitting tensile strength, and age at cracking under restrained shrinkage on average by 55%, 27%, and 69%, respectively.

TABLE OF CONTENTS

LIST OF TABLES

LIST OF FIGURES

CHAPTER 1

INTRODUCTION

1.1. POLYMER-MODIFIED MORTARS

Polymer-modified mortars (PMMs) are ordinary Portland cement composites in which either a monomer or a polymer is added to the fresh mixture in liquid, powdery, or dispersed phase, and subsequently allowed to cure, and if needed, polymerize in place [1]. During hardening and curing of a PMM, cement hydration and polymer film formation take place resulting in a co-matrix in which the polymer film is intermingled with cement hydrates. The mixing proportions and procedures are similar to those for conventional cement mortar mixtures but curing differs as only one to two days of moist curing are required, followed by air curing. Polymers are typically added in polymer-cement (p/c) weight ratios of 5% to 20% and lead to improvements in workability, setting time, adhesion, strength, and durability [2-5].

1.2. PROPERTIES OF PMMS

PMMs exhibit enhanced workability due to: (1) the “ball bearing” action of polymer particles, (2) air-entraining (3) the dispersing effects of surfactants present in latexes [6]. This property makes PMMs attractive for crack filling and patching applications, and facilitates mortar placement under difficult conditions [7]. The incorporation of polymers can result either in an acceleration [8] or deceleration of cement hydration [9], depending on the type of polymer, and therefore are used in a wide range of environments and applications. The use of polymeric binders in conjunction with cement can significantly improve mortar adhesion to concrete substrates [10-13] and embedded reinforcement [14, 15] for

strengthening and repair purposes. For example, it was shown that replacing 15% of cement with styrene-butadiene rubber (SBR), polyacrylic ester (PAE), and poly (vinylidene chloride-vinyl chloride) (PVDC) led to an increase in the bond strength of mortar to a concrete substrate by 100%, 60% and 60%, respectively [16].

Most PMMs exhibit lower compressive strength [17, 18] and rigidity [19] than counterpart cement mortars due to low rigidity of polymer particles [20]. However, since polymers are typically stronger and more deformable in tension [21] than cement paste [22], the tensile strength [19] and flexural strength [18-20, 23] are significantly higher for PMMs. Strength and deformability enhancements is associated with the following mechanisms:

(1) Polymers function as water-reducers enabling relatively high slumps at low w/c ratios [17]. As a consequence of low water content, fewer voids are formed and stronger composites are obtained.

(2) Polymers reduce the porosity by filling in cavities and capillaries resulting in a denser microstructure [24, 25].

(3) The incorporation of polymers may also promote cement hydration through a ‘water-retention’ effect. Water is entrapped in the PMM matrix as it forms [8] resulting in a more effective cement hydration [26]. Several researchers correlated enhancements in mechanical properties to alterations in the amount and morphology of different hydration products such as $Ca(OH)_2$ and ettringite due to polymer incorporation [8, 9, 24, 26].

(4) Surfactants present in polymers neutralize the surface charges on cement particles enhancing their dispersion in water, and this results in the formation of a more homogenous material, that is, containing fewer defects or relatively weaker areas [4].

(5) In polymer-cement matrices, polymer membranes participate in the formation of a network throughout the matrix in conjunction with the cement phase [24, 27]. Figure 1.1 presents the widely-accepted model of formation of polymer-cement matrix proposed by Ohama [2]. Partial or full encapsulation of cement paste and aggregates, physical interlock, and interface adhesion provide local confinement for the increasing the load-bearing capacity of PMMs compared with counterpart cement mortars [4]. Polymers may also form chemical bonds with hydrates further improving the interface bond strength [9, 28].

(6) Polymers enhance the interface strength between aggregates and matrix by improving adhesion and enhancing the interfacial transition zone (ITZ) [12]. In fact, previous findings show that both the thickness and porosity of ITZ can be reduced [4, 28, 29]. For example, Rossignolo [29] reported that the addition of 5% and 10% of SBR decreased the thickness of the interface transition zone (ITZ) by 27% and 36%, respectively.

(7) Polymers can also bridge defects and cracks at different scales and increase the toughness and damage tolerance of mortar [13, 26]. In particular, toughness enhancement can be partially attributed to the viscoelastic behavior of polymers which also improves the vibration

damping capacity of PMMs [14]. Crack-bridging effect of PAE and poly(ethylene-vinyl acetate) (PEVA) in PAE- and EVA-cement mortar is illustrated in Figure 1.2.

Another advantage PMMs offer over plain mortar is improved durability. Due to their dense microstructure, PMMs have comparatively lower permeability and water absorption [4, 10, 17, 23]. Consequently, the resistance to a wide range of aggressive agents such as acids, salts, oxygen, CO_2, chloride ions, and sulfate ions is much higher for these composites [10, 17, 19, 23, 27, 30]. Freeze-thaw resistance is also improved [17]. Due to their water-reducing and water-retention effects, PMMs are typically made with relatively low w/c ratios (i.e., in the range 0.25-0.40 compared with 0.4-0.6 in cement mortars) and therefore undergo smaller drying shrinkage [19]. Moreover previous research reported on the protective effect of cement-polymer matrices against corrosion of steel reinforcement as a result of the reduced permeability [31].

However, there are also drawbacks associated with the use of PMMs as higher p/c ratios are used. One limitation is the relatively high cost of polymers [3]. Another limitation is the vulnerability of polymers against UV radiation [30] and high temperatures [10]. Polymers may also re-emulsify in humid alkaline conditions [23] and water-soluble polymers may undergo degradation when

exposed to water for long periods of time [32]. Moreover, some polymers are highly vulnerable to specific chemicals. For example five cycles of 7-day immersion of epoxy resin-cement mortar specimens in formic acid decreased the flexural and compressive strengths, by 85% and 56%, respectively [30]. Other drawbacks regarding storage, handling, and disposal of polymers include odor, toxicity, flammability, and combustibility [30]. Therefore, finding ways to offset these drawbacks and maintain the advantages PMMs can offer is of significance in the context of infrastructure maintenance and sustainability.

1.3. APPLICATIONS OF PMMS

The combination of improved workability, durability, adhesion, and curing performance allows using PMMs in patch and repair applications as well as structural and protective overlays. The enhanced workability of PMMs improves application characteristics of PMMs especially in crack-filling applications [17]. The low drying shrinkage of PMMs due to water retention effect of polymers is of great importance in thin application where the surface area relative to the mortar volume is high [19]. In hot climates, the use of polymers that prolong the working time facilitates handling and application of repair mortar. The rapid setting property of PMMs makes them suitable for overhead applications. Since most PMMs do not require long periods of wet curing, they can be used in repair applications at locations where access is difficult for water curing. Improved adhesion of PMMs enables the repair mortar to stick to a wide range of surfaces such as concrete, masonry, brick, wood, glass and metals [10-13].

1.4. DOPAMINE

In this thesis, mussel-inspired dopamine (DA) is introduced as a potential monomer additive to manufacture high-strength and low-shrinkage PMM with p/c ratios one order of magnitude smaller than typical values. First synthesized in 1910 by Georg Barger and James Ewen, DA or 3,4-dihydroxyphenethylanine, is a simple organic molecule that consists of a catechol structure (a benzene ring with two hydroxyl side groups) with one amino group attached, both of which are considered the main contributors to versatile adhesiveness of mussels [33]. Figure 1.3 shows a common blue mussel hanging to a non-stick Teflon surface. In a weak alkaline aqueous solution, DA self-polymerizes to form ultra-thing (20-65 nm) layers of poly(dopamine) (PDA) that adheres to virtually all types of organic and inorganic substrates under wet and dry conditions [33]. A very limited literature exists on the bond strength of PDA to different material. Yang and Zhao [34] investigated the bonding of PDA-coated aluminum to glass and polydimethylsiloxane (PDMS) (a silicon-based organic polymer) and observed that the failure of adhesive bonds happened within the PDA layer rather than at the interfaces suggesting strong bonding was formed. The bond strength between aluminum coated with PDA aqueous solution with concentration of 4 mg/ml was found to be 25,000 Pa and 10,000 Pa, for glass and PDMS, respectively.

The investigation reported herein drew from the adhesion properties and ultra-thinness of PDA films compared with film thickness of conventional

polymers. For example latex, polyvinyl alcohol (PVA), and cellulose ether (CE) form films with associated thickness of around 1-4 μm [12]. It was envisioned that due to the nano-size thickness of PDA membranes an effective polymer network can be formed using small amounts of polymeric binder. Knapen and Van Gemert [26] showed that certain polymers even at p/c ratios as small as 0.01 can effectively form PDA films in cement matrices improving the mechanical performance of the resulting cement mortar. In this study, prototype PDA-cement mortars were manufactured using PDA amounts of 0.1, 0.2, and 0.5 wt%, and then characterized based on the compressive and splitting tensile strength, and the restrained drying shrinkage. The microstructure was examined by means of scanning electron microscopy and energy-dispersive X-ray spectroscopy (SEM/EDX) analysis to shed light on the mechanisms of strength and deformability enhancements attributed to the addition of PDA.

1.5. REFERENCES

[1] ACI Committee 548. Report on polymer-modified concrete. Farmington Hills, MI: American Concrete Institute 2009.

[2] Ohama Y. Handbook of polymer-modified concrete and mortars: properties and process technology. Koriyama (Japan): Noyes Publications 1995.

[3] Fowler DW. Polymers in concrete: a vision for the 21st century. Cement Concrete Comp 1999; 21(5): 449-452.

[4] Kardon JB. Polymer-modified concrete: review. J Mater Civil Eng 1997; 9(2): 85-92.

[5] Van Gemert D, Czarnecki L, Maultzsch M, Schorn H, Beeldens A, Łukowski P, and Knapen E. Cement concrete and concrete–polymer composites: Two merging worlds: A report from 11th ICPIC Congress in Berlin, 2004. Cement Concrete Comp 2005; 27(9): 926-933.

[6] Salomone JC (Ed). Concise polymeric materials encyclopedia. CRC press 1999; 1: 278-281.

[7] Allen RTL, Edwards SC, and Shaw DN. Repair of concrete structures. Taylor & Francis 1992.

[8] Wang R, Li XG, and Wang PM. Influence of polymer on cement hydration in SBR-modified cement pastes. Cement Concrete Res 2006; 36(9): 1744-1751.

[9] Silva DA, Roman HR, and Gleize PJP. Evidences of chemical interaction between EVA and hydrating Portland cement. Cement Concrete Res 2002; 32(9): 1383-1390.

[10] Al-Zahrani MM, Al-Dulaijan SU, Ibrahim M, Saricimen H, and Sharif FM. Effect of waterproofing coatings on steel reinforcement corrosion and physical properties of concrete. Cement Concrete Comp 2002; 24(1): 127-137.

[11] Afridi MUK, Ohama Y, Zafar Iqbal M, and Demura K. Water retention and adhesion of powdered and aqueous polymer-modified mortars. Cement Concrete Comp 1995; 17(2): 113-118.

[12] Jenni A, Holzer L, Zurbriggen R, and Herwegh M. Influence of polymers on microstructure and adhesive strength of cementitious tile adhesive mortars. Cement Concrete Res 2005; 35(1): 35-50.

[13] Sakai E, and Sugita J. Composite mechanism of polymer modified cement. Cement Concrete Res 1995; 25(1): 127-135.
[14] Chung DDL. Use of polymers for cement-based structural materials. J Mater Sci 2004; 39(9): 2973-2978.

[15] Fu X, and Chung DDL. Effect of polymer admixtures to cement on the bond strength and electrical contact resistivity between steel fiber and cement. Cement Concrete Res 1996; 26(2): 189-194.

[16] Ohama Y. Study on properties and mix proportioning of polymer modified mortars for buildings. Report of the Building Research Institute 1973; 65: 170.

[17] Saija LM. Waterproofing of Portland cement mortars with a specially designed polyacrylic latex. Cement Concrete Res 1995; 25(3): 503-509.

[18] Barluenga G, and Hernández-Olivares F. SBR latex modified mortar rheology and mechanical behaviour. Cement Concrete Res 2004; 34(3): 527-535.

[19] Al-Zahrani MM, Maslehuddin M, Al-Dulaijan SU, and Ibrahim M. Mechanical properties and durability characteristics of polymer-and cement-based repair materials. Cement Concrete Comp 2003; 25(4): 527-537.

[20] Pascal S, Alliche A, and Pilvin P. Mechanical behaviour of polymer modified mortars. Mater Sci Eng A 2004; 380(1): 1-8.

[21] ACI Committee 503. Guide for the selection of polymer adhesives with concrete. Farmington Hills, MI: American Concrete Institute 2003.

[22] Brandt AM. Cement-based composited: materials, mechanical properties and performance. New York: Taylor & Francis, 2009.

[23] Aggarwal LK, Thapliyal PC, and Karade SR. Properties of polymer-modified mortars using epoxy and acrylic emulsions. Constr Build Mater 2007; 21(2): 379-383.

[24] Yang Z, Shi X, Creighton AT, and Peterson MM. Effect of styrene–butadiene rubber latex on the chloride permeability and microstructure of Portland cement mortar. Constr Build Mater 2009; 23(6): 2283-2290.

[25] Silva DA, John VM, Ribeiro JLD, and Roman HR. Pore size distribution of hydrated cement pastes modified with polymers. Cement Concrete Res 2001; 31(8): 1177-1184.

[26] Knapen E, and Van Gemert D. Cement hydration and microstructure

formation in the presence of water-soluble polymers. Cement Concrete Res 2009; 39(1): 6-13.

[27] Afridi MUK, Ohama Y, Demura K, and Iqbal MZ. Development of polymer films by the coalescence of polymer particles in powdered and aqueous polymer-modified mortars. Cement Concrete Res 2003; 33(11): 1715-1721.

[28] Gao JM, Qian CX, Wang, B and Morino K. Experimental study on properties of polymer-modified cement mortars with silica fume. Cement Concrete Res 2002; 32(1): 41-45.

[29] Rossignolo JA. Interfacial interactions in concretes with silica fume and SBR latex. J Constr Build Mater 2009; 23(2): 817-821.

[30] Reis JML. Mechanical characterization of polymer mortars exposed to degradation solutions. Constr Build Mater 2009; 23(11): 3328-3331.

[31] Nepomuceno AN, and Andrade C. Steel protection capacity of polymeric based cement mortars against chloride and carbonation attacks studied using electrochemical polarization resistance. Cement Concrete Comp 2006; 28(8): 716-721.

[32] Jenni A, Zurbriggen R, Holzer L, and Herwegh M. Changes in microstructures and physical properties of polymer-modified mortars during wet storage. Cement Concrete Res 2006; 36(1): 79-90.

[33] Lee H. Mussel-inspired surface chemistry for multifunctional coatings. Science 2007; 318(5849): 426-430.

[34] Yang FK, Zhao B. Adhesion Properties of Self-Polymerized Dopamine Thin Film. Open Surf. Sci. J 2011; 3: 115-122.

1.6. FIGURES

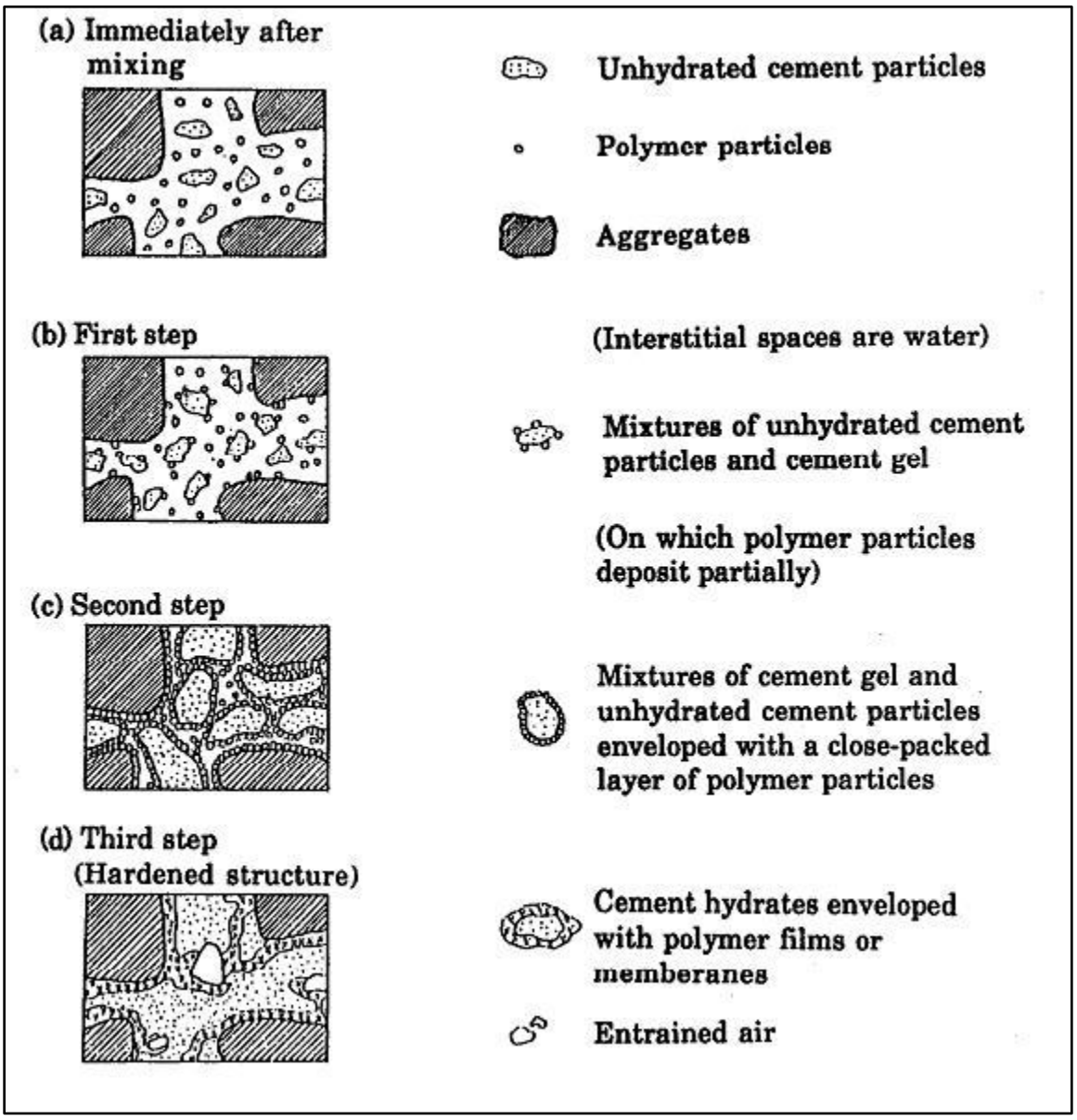

Figure 1.1 - Simplified model of formation of polymer-cement co-matrix [2]

(a)

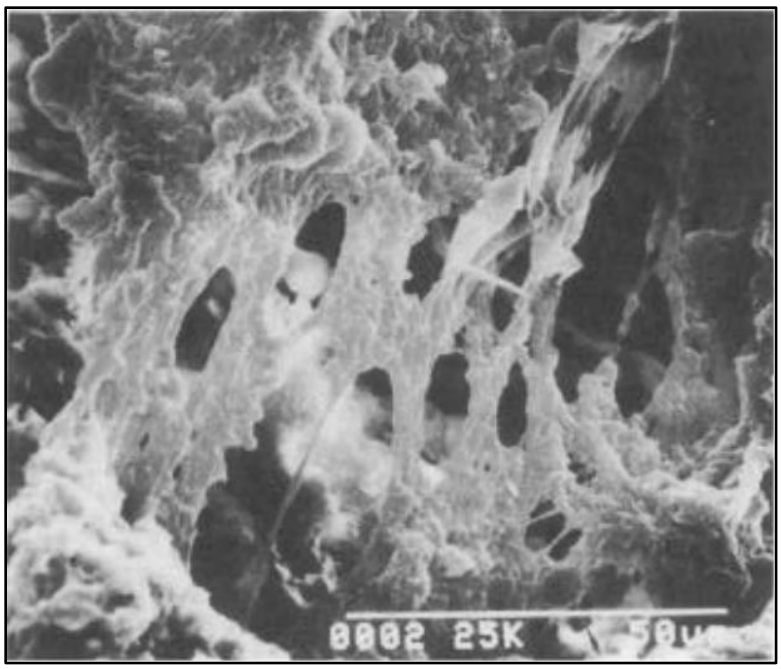

(b)

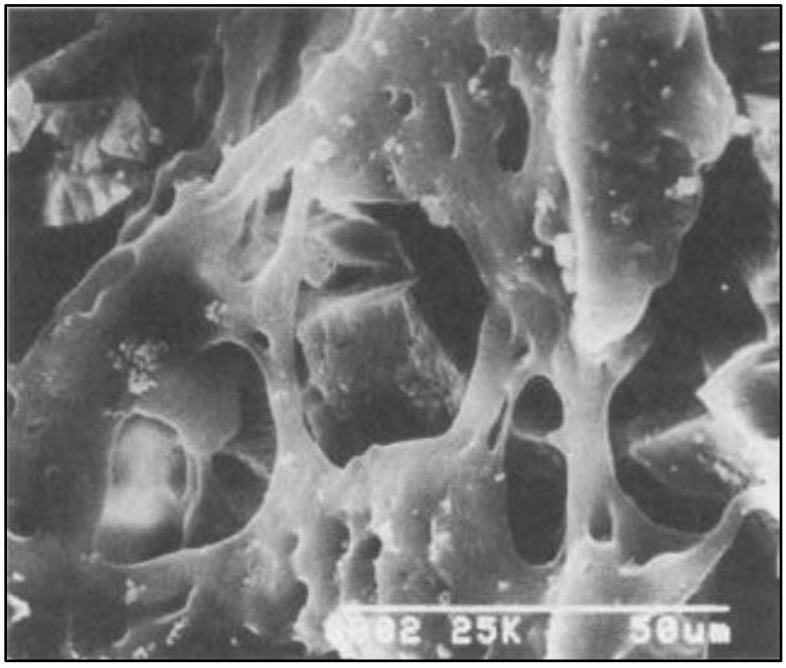

Figure 1.2 - SEM micrographs illustrating the crack-bridging effect of polymers in PMMs: (a) EVA-cement mortar, (B) PAE-cement mortar

Figure 1.3 - Common blue mussel (Mytilus edulis) hanging from “non-stick” Teflon surface. (Credit: Jonathan Wilker of Purdue University, National Science Foundation (NSF))

CHAPTER 2

EXPERIMENTAL PROGRAM

2.1. MATERIALS

Ordinary Portland cement (OPC) Type I and standard silica sand in accordance with ASTM C778 were used for all specimens [1]. The grading curve of the sand used is presented in Figure 2.1. DA was purchased in the form of dopamine hydrochloride, a white powder with a chemical formula of $C_8H_{11}NO_2$.HCl (Sigma Aldrich, St. Louis, Missouri, cat# H8502), and was used as-received. The DA material specifications provided by the supplier are presented in Table 2.1. Since DA is highly reactive it is often supplied in the form of dopamine hydrochloride to prevent undesirable reactions.

2.2. PREPARATION OF PDA MORTAR

The DA was first dispersed in water and the resulting solution was immediately mixed with cement and sand following ASTM C305 [2]. A pH level of 8.5 is required to activate the DA polymerization process [3]. Prior to the addition of DA, the pH was measured using a digital pH-meter (Orion 8102BNUWP Ross Ultra Combination pH, Thermoscientific, Rochester, NY) and raised to 8.5 by adding suitable amounts of 1 M sodium hydroxide solution, NaOH (Sigma Aldrich, cat# 221465). In addition, pH changes must be minimized during the polymerization process to enable a continuous and stable progress. A 10 mM TRIS buffer solution has been found effective in maintaining a stable and suitable pH level [4]. A buffer is an aqueous solution consisting of a mixture of a weak acid and its conjugate base, or a weak base and its conjugate acid. In a buffer solution, the pH undergoes negligible changes when a small amount of strong

acid or base is added to it and thus it is used to maintain a stable pH. TRIS buffer solutions were prepared by adding TRIS buffered saline (Sigma Aldrich, cat# T5912) to deionized water at a volume ratio of 19:1. Then, the DA was dispersed in TRIS aqueous solutions by magnetic stirring for one minute using a VWR magnetic stirrer (Henry Troemner LLC, Thorofare, New Jersey). Dopamine hydrochloride is water soluble and thus dispersion in the solution was easily achieved. The preparation steps of PDA mortar are summarized in Figure 2.2.

2.3. CHARACTERIZATION OF DA POLYMERIZATION

The mechanism by which small DA particles coalesce into PDA films is still under debate. The predominant view is that in alkaline environments DA undergoes self-polymerization where the catechol structure is oxidized and subsequently cross-linked to form PDA films or membranes [5]. Another view is that DA membrane is not a covalent polymer but instead a supramolecular aggregate of monomers that are held together through a combination of charge transfer, π-stacking, and hydrogen bonding interactions [6]. Whether a polymer or an amorphous aggregate, in this study DA deposition process is referred to as DA polymerization and the deposition product is referred to as poly(dopamine) or PDA.

The DA polymerization in TRIS buffer solution was characterized by applying time-resolved dynamic light scattering (TRDLS). In this technique a laser light is beamed through the DA aqueous sample. When the light hits the DA

particles it scatters in all directions. Due to random Brownian motion of particles, the intensity of the scattered light fluctuates in time. These fluctuations are correlated with the hydrodynamic radius of the particles providing information on the PDA coil size in the solution. As DA polymerizes, the DA particles coalesce into larger particles with larger hydrodynamic radii. Therefore the average hydrodynamic radius (AHR) of the DA particles was estimated over time to monitor the polymerization process.

The AHR measurements were conducted using an ALV/CGS-3 compact goniometer system (ALV-Laser Vertriebsgesellschaft m-bH, Langen/Hessen, Germany). The TRDLS system was equipped with a 22 mW HeNe Laser at 632 nm wavelength and high QE APD detector with photomultipliers of 1:25 sensitivity. DA solutions of 4 mg/mL concentration were prepared. A cleaned borosilicate glass vial was filled with 2 mL polymer suspension and vortex mixed prior to insertion into the TRDLS vat chamber. Continuous data collection at 15 second intervals was performed for up to 10 minutes with the laser operating at full exposure level, and scattering data collected at a 90° scattering.

The stability of the polymerization process was investigated by visually inspecting the DA solutions during the first 24 hours after dispersion. The inspections were documented by taking photographs of the solution.

2.4. COMPRESSIVE STRENGTH

The prototype PDA mortars were first characterized based on the 7-day and 28-day compressive strength. As will be seen in chapter 3, the compressive strength and its consistency (i.e., comparable or better standard deviation vis-à-vis the counterpart cement mortar) provide useful information on the development of an effective polymer network in the PDA-cement mortar. In addition, key mechanical properties such as tensile strength and Young's modulus are typically correlated with the compressive strength and thus follow its trend. Three p/c ratios of 0.1, 0.2, and 0.5% were considered. Five samples per group were tested following ASTM C109 [7]. The 2-in. cube specimens were moist-cured for 24 hours, demolded, and cured in saturated lime water until the age of 28 days. Compression tests were performed using a test frame (MTS 810 Material Testing System, MTS systems Inc., Eden Prairie, Minnesota) under displacement control mode with a displacement rate of 0.625 mm/minute. It was noted at the time of mixing that addition of DA increased the workability (flow) of the mixtures, but also significantly reduced the setting time. In fact, the fresh mixtures containing DA began to set in about 10 minutes after mixing. Photographs of specimens and test setup are presented in Figure 2.3.

2.5. SPLITTING TENSILE STRENGTH

Apart from the flexure test the other methods to determine the tensile strength of concrete can be broadly classified as (a) direct methods, and (b) indirect methods. Direct methods suffer from a number of difficulties related to

holding the specimen properly in the test machine without introducing stress concentration, and to the application of uniaxial tensile load preventing any eccentricity. As mortar is relatively weak in tension, even small eccentricities would produce combined bending and axial force, resulting in premature failure at an apparent tensile stress that is smaller than the actual tensile strength.

As there are many difficulties associated with the direct tension test, a number of indirect methods have been developed to determine the tensile strength. In these tests in general a compressive force is applied to a concrete specimen in such a way that the specimen fails due to indirect tensile stresses. The splitting tensile strength test or Brazilian test is a well-known indirect test used for determining the splitting tensile strength of concrete (per ASTM C496 [8]) and cement composites in general. The test consists of applying a compressive line load along the length of a concrete cylinder placed with its longitudinal axis parallel to the loading platens. The compressive load produces a fairly uniform tensile stress over approximately 2/3 of the cylinder diameter as obtained from an elastic analysis. Figure 2.4 shows a schematic view of a cylinder specimen together with the induced stress profile, and photographs of specimens before and after the tests.

Three p/c ratios, 0%, 0.2% and 0.5%, were considered. The DA aqueous solutions containing the two different amounts of DA were mixed with cement and sand in cement:sand:solution weight proportions of 1:2.75:0.5. Five cylinder

specimens of 75 mm in diameter and 150 mm in height were cast per mix design. The specimens were demolded and tested after 28 days.

Before testing, diametrical lines were drawn on two ends of the specimen so that they lied in the same axial plane. The diameter and length of the specimens were measured to the nearest 0.2 mm. Each specimen was placed on the plywood strip and aligned so that lines marked on the end of the specimen were vertical and centered over the plywood strip. The second plywood strip was placed length wise on the cylinder centered on the lines marked on the ends of the cylinder. The load was applied at a rate of between 1.4 and 2.1 MPa/min till failure. The tensile strength values were calculated to the nearest 0.25 MPa.

2.6. RESTRAINED DRYING SHRINKAGE

Drying shrinkage is the time-dependent deformation caused by the loss of water from the network of capillary pores within the hardened mortar matrix. The main mechanisms by which the water loss causes volume reduction are: (1) disjoining pressure, (2) capillary stress, and (3) surface free energy [9]. Disjoining pressure is the pressure caused by water in small gaps of the capillary pores. When water evaporates this pressure is reduced and the cement paste particles are drawn closer which results in shrinkage. Capillary stress occurs when a meniscus is formed on the water in partially-filled pores. The meniscus is under hydrostatic tension and exerts a hydrodynamic compression on the surrounding cement paste. This compressive stress reduces the size of the capillary pores,

and thus the overall volume of the cement paste. Variations of the surface free energy also contribute to mortar shrinkage. The outermost layers of water surrounding cement particles are the most strongly adsorbed. This water has a high surface tension and places cement particles under a compressive force, reducing the cement paste volume [10].

When the mortar is placed under restraining boundary conditions, such as in the case of a repair patch or overlay bonded onto a concrete substrate, restrained shrinkage results in tensile stresses in the mortar. As drying progresses, the tensile stress increases and shrinkage cracking occurs when the tensile stress reach the tensile strength of the mortar. Several test methods with different specimen geometries and boundary conditions have been proposed and developed to characterize stresses and cracking in restrained shrinkage conditions. The most common test methods have used flat specimens, plate-type specimens, and ring specimens [11-15].

In the restrained ring test per ASTM C1581 [16], a mortar ring is cast around an inner steel ring. The steel ring restrains the shrinking mortar, producing an internal pressure on the ring, which causes tensile hoop stresses to develop in the mortar. When the tensile stresses exceed the tensile strength of the mortar, cracking occurs. The steel ring is instrumented to monitor the strain development and determine the age of cracking. Figure 2.5 presents a schematic and a photograph of the test setup used in this study.

The effect of PDA on the restrained shrinkage of PDA-cement mortar was studied using the ASTM C1581 ring test [17]. Three p/c ratios of 0%, 0.2% and 0.5% were considered. The mixing proportions were the same as those used for the splitting tensile test specimens. Three identical ring specimens were cast per p/c ratio. Three electrical strain gages were mounted at the mid-height of each steel ring, distanced equally from each other. The outer PVC rings were removed after 24 hours and the top surfaces of the specimens were sealed using silicon sealant. All specimens were stored in the same environmental conditions at a 50% RH and 21^{o}C temperature. The test was terminated after 28 days and the crack widths were measured with a crack-detection optical microscope that had 0.02-mm divisions, 35X magnification, and a built-in light source (EI35-2505, ELE International, Loveland, CO).

2.7. SEM AND EDX ANALYSIS

The morphology and microstructure of the PDA-cement matrix were studied using SEM and EDX analysis. The SEM analysis was performed using a Zeiss Ultra Plus Field Emission Scanning Electron Microscope (FESEM). Samples were collected from fracture surfaces of failed specimens. All samples were oven dried for 24 hours at 60^{o}C and gold sputtered prior to being examined.

2.8. REFERENCES

[1] ASTM Standard C778 2013. Standard specification for standard sand. ASTM International, West Conshohocken, PA, 2013, DOI: 10.1520/C0778, www.astm.org.

[2] ASTM Standard C305 2013. Standard practice for mechanical mixing of hydraulic cement pastes and mortars of plastic consistency. ASTM International, West Conshohocken, PA, 2013, DOI: 10.1520/C0305, www.astm.org.

[3] Han G, Zhang S, Li X, Widjojo N, and Chung TS. Thin film composite forward osmosis membranes based on polydopamine modified polysulfone substrates with enhancements in both water flux and salt rejection. Chem Eng Sci 2012; 80: 219-231.

[4] Liao Y, Cao B, Wang WC, Zhang L, Wu D, Jin R. A facile method for preparing highly conductive and reflective surface-silvered polyimide films. Appl Surf Sci 2009; 255(19): 8207-8212.

[5] Li B, Liu W, Jiang Z, Dong X, Wang B, Zhong Y. Ultrathin and stable layer of dense composite membrane enabled by poly(dopamine). Langmuir 2009; 25(13): 7368-7374.

[6] Dreyer DR, Miller DJ, Freeman BD, Paul DR, Bielawski CW. Elucidating the structure of poly(dopamine). Langmuir 2012; 28(15): 6428-6435.

[7] ASTM Standard C109/C109M 2013. Standard test method for compressive strength of hydraulic cement mortars (Using 2-in. or [50-mm] cube specimens). ASTM International, West Conshohocken, PA, 2013, DOI: 10.1520/C0109_C0109M, www.astm.org.

[8] ASTM Standard C496/C496M 2011. Standard test method for splitting tensile strength of cylindrical concrete specimens. ASTM International, West Conshohocken, PA, 2011, DOI: 10.1520/C0496_C0496M-11, www.astm.org.

[9] Hansen W. Drying shrinkage mechanisms in Portland cement paste. J Am Ceram Soc 1987; 70(5): 323-328.

[10] Tritsch N, Darwin D, and Browning JA. Evaluating shrinkage and cracking behavior of concrete using restrained ting and free shrinkage tests. In

Structural Engineering and Engineering Materials SM report No. 77; The University of Kansas Center for Research; 2005.

[11] Hossain AB, and Weiss J. Assessing residual stress development and stress relaxation in restrained concrete ring specimens. Cement and Concrete Comp 2004; 26(5): 531-540.

[12] Filho RDT, Ghavami K, Sanjuán MA, and England GL. Free, restrained and drying shrinkage of cement mortar composites reinforced with vegetable fibres. Cement and Concrete Comp 2005; 27(5): 537-546.

[13] Pease B, Shah H, and Weiss J. Shrinkage behavior and residual stress development in mortar containing shrinkage reducing admixtures (SRAs). ACI Special Publication 227 (2005).

[14] McLaskey GC, Glaser SD, and Grosse CU. Integrating broad-band high-fidelity acoustic emission sensors and array processing to study drying shrinkage cracking in concrete. In The 14th International Symposium on: Smart Structures and Materials & Nondestructive Evaluation and Health Monitoring, pp. 65290C-65290C. International Society for Optics and Photonics, 2007.

[15] Shah HR, and Weiss J. Quantifying shrinkage cracking in fiber reinforced concrete using the ring test. Mater Struct 2006; 39(9): 887-899.

[16] ASTM Standard C1581/C1581M 2009a. Standard test method for determining age at cracking and induced tensile stress characteristics of mortar and concrete under restrained shrinkage. ASTM International, West Conshohocken, PA, 2009, DOI: 10.1520/C1581_C1581M-09A, www.astm.org.

2.9. TABLES

Table 2.1- Material specifications for dopamine hydrochloride

Color	Molecular weight [g/mol]	Melting point [^{o}C]	Solubility	Storage temperature [^{o}C]
Light tan	189.64	248 - 250	H_2O soluble	2 - 8

2.10. FIGURES

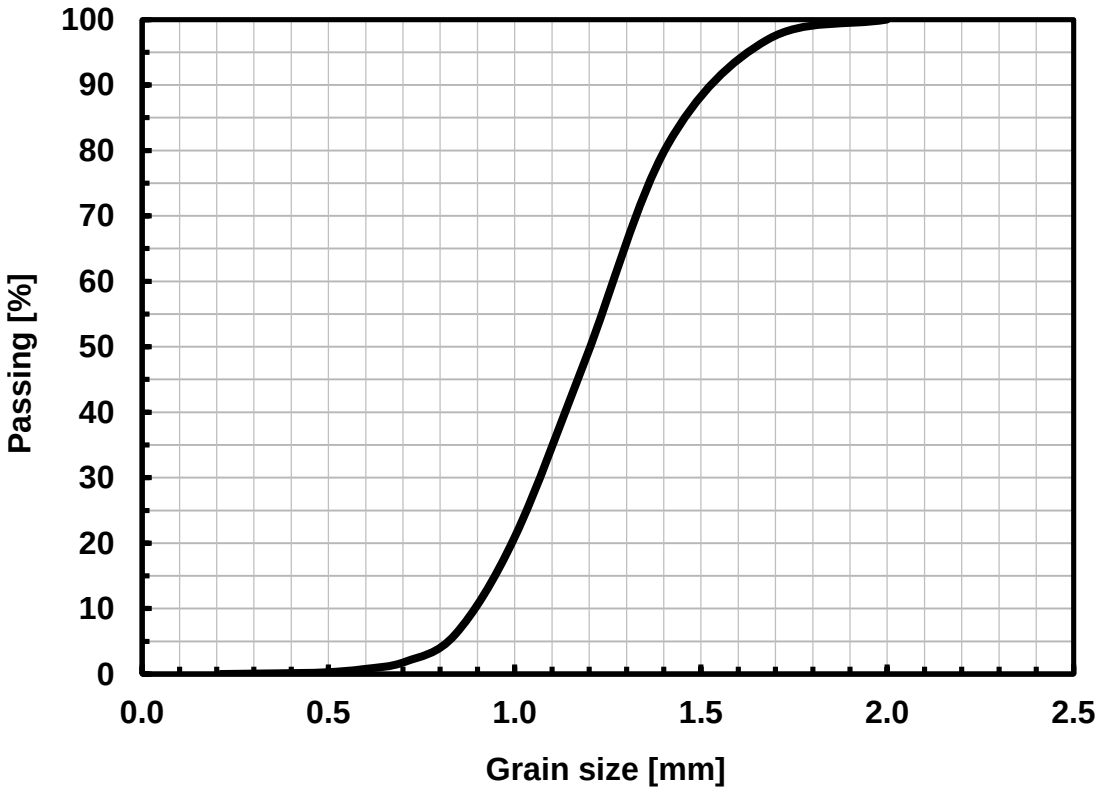

Figure 2.1 - Grading curve for the sand used in all experiments

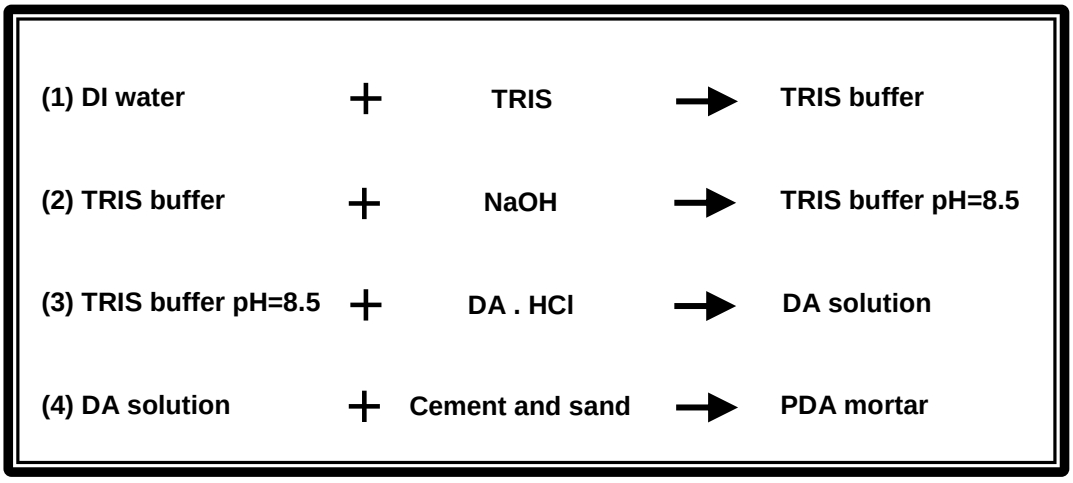

Figure 2.2 - Preparation steps of PDA mortar

Figure 2.3 - Photographs of compression specimens and tests: (a) moist-curing of cube specimens; (b) cube specimen under compressive load, (c) failed cube specimen, (d) failed specimens

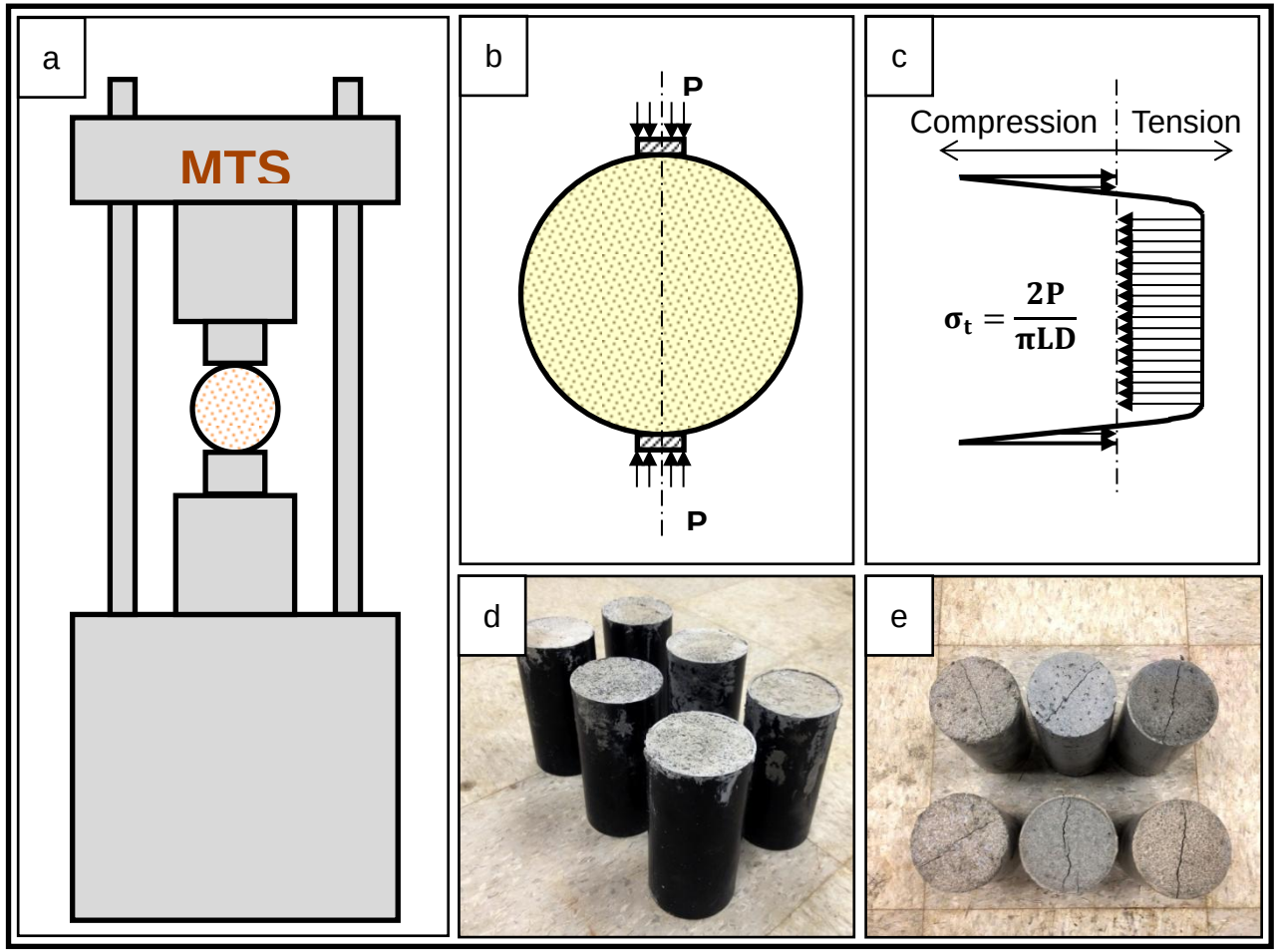

Figure 2.4 – Splitting tensile test: (a) schematic view of test setup, (b) schematic view of cylinder specimen under compressive load, (c) stress profile in cylinder specimens, (d) unmolded mortar cylinders, (e) failed specimens

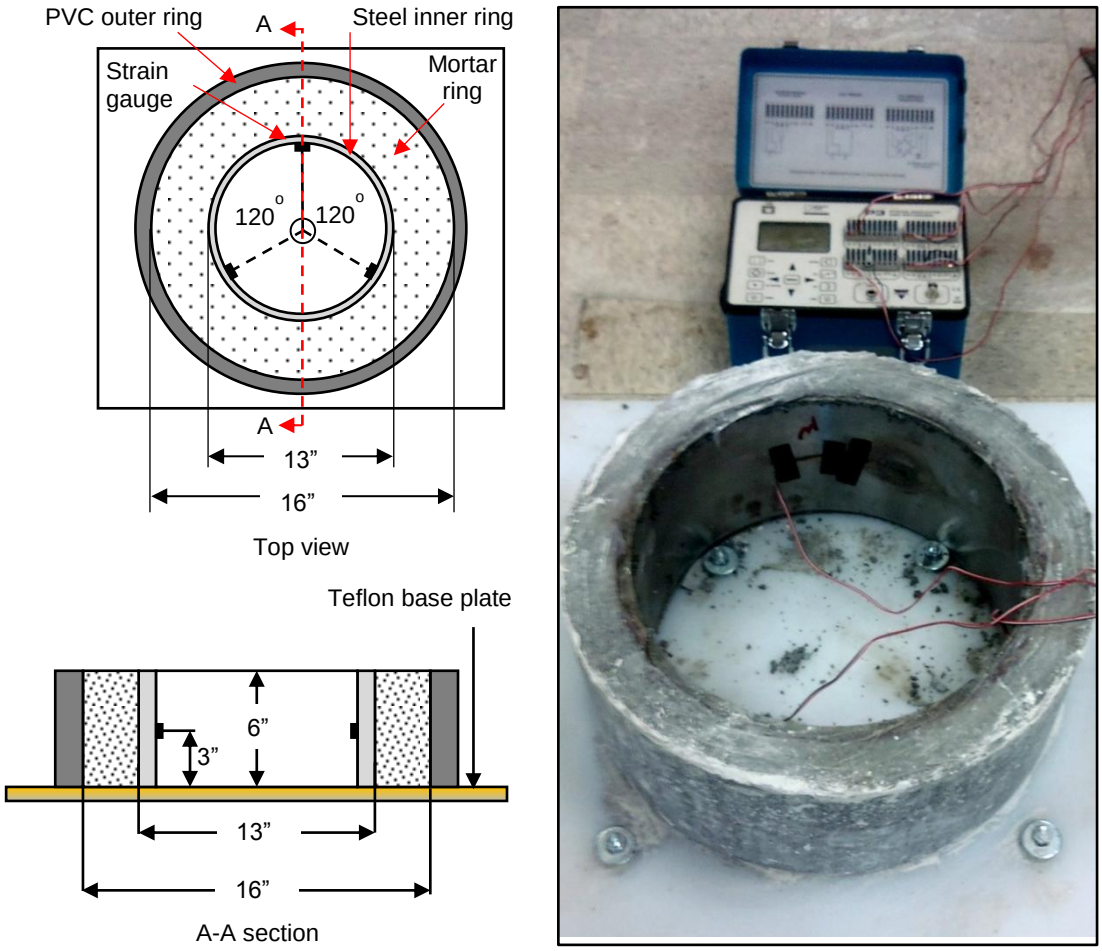

Figure 2.5 - Schematic and photograph f restrained shrinkage test setup

CHAPTER 3

RESULTS AND DISCUSSION

3.1. DA POLYMERIZATION

The DA polymerization was characterized by means of TRDLS analysis and visual inspections of PDA solutions. Variations in the AHR of polymer particles in aqueous solution in the first 7 minutes after mixing are shown in Figure 3.1. In the first 7 minutes the average PDA coil size almost doubled highlighting the initiation of the polymerization process. The stability of the polymerization process was verified by visual inspections of DA solutions during the first 24 hours after dispersion. The inspections were documented by taking photographs of the solutions. Figure 3.2 shows photographs taken immediately after dispersion, at 15 minutes, 3 hours, and 24 hours after dispersion. The color of the solution darkened gradually indicating a progressive oxidation process [1]. After 3 hours larger polymer particles were visible by eye as dark spots in the solution. The PDA formation can be visualized by noting the formation of a black coating on the white stir bar at the bottom of the container at 24 hours. The side parallel to the deposition direction remained un-coated.

3.2. EFFECT OF PDA ON COMPRESSIVE STRENGTH

The measured compressive strength and standard deviation for plain and PDA mortar are presented in Table 3.1. The average compressive strength increased nearly linearly with the p/c ratio (Figure 3.3). In addition, the modified samples showed similar and in most cases smaller standard deviations compared with control samples suggesting that an effective formation and distribution of PDA throughout the composite matrix was achieved. Conventional

PMMs typically exhibit smaller compressive strength than plain mortar due to incorporation of soft polymer particles [2-4]. This empirical evidence suggests that the amounts of polymer used in this study were small enough to positively affect the compressive strength through the formation of an effective PDA-cement matrix, as discussed in the following section.

3.3. EFFECT OF PDA ON MICROSTRUCTURE

3.3.1. MICROSTRUCTURE

It is well established that the microstructure of cement composites greatly affects their mechanical properties [5]. The microstructure of PDA-cement composites was characterized through SEM and EDX analysis of fracture surfaces from failed specimens. A representative SEM micrograph illustrating the typical microstructure of PDA-cement mortar is presented in Figure 3.4. Polymerization products may appear as mesh-like, thread-like, rugged, dense, or fibrous, with either relatively fine or rough surfaces [6]. Therefore distinguishing between polymer and cement hydrates especially at low p/c ratios (1-4%) can be very difficult [5]. The black PDA particles observed in aqueous solutions (Figure 3.2) appeared in the PDA-cement composite matrix as continuous and dense membranes. The PDA morphology was verified using EDX analysis. The X-ray spectrum of point A in Figure 3.4 is presented in Figure 3.5. A clear carbon peak at around 0.28 keV was recorded. Since PDA films are the only source of carbon atoms in the matrix, the structure at point A was confirmed as PDA. This conclusion was validated by quantitative elemental analysis along line BC in

Figure 3.4. Variations of carbon atomic concentration were collected along the line. The line was drawn such that it passed across both cement paste and the structure assumed to be a PDA film. The locations where the line intersects the assumed PDA film are marked with arrows in the figure. The sharp increase in carbon concentration at the locations of assumed PDA confirms the previous conclusion. The microstructure of PDA mortar is similar to that of latex-modified mortars where a polymer phase appears as a network of polymer films or membranes throughout the cement phase [7]. Such structure can be rendered as a matrix combined of nano- to micro-scale irregular cement paste cells separated by PDA films. This polymer network is the origin of strength enhancements [4]. In the present case, the strength enhancement mechanisms are discussed below.

3.3.2. LOCAL CONFINEMENT

In the PDA-cement matrix, PDA films extend over mortar constituents encapsulating them to different extents as illustrated in Figure 3.6-a. Encapsulating films restrain the deformation of cement hydrates under stress, thus creating a physical confinement for cement paste cells at a local level. If an effective network of PDA films is formed throughout the composite the effects of local confinement can enhance the load-bearing capacity and deformability. Figure 3.6-b shows the marked PDA films in Figure 3.6-a, at a higher magnification. It can be seen that the PDA film has deformed, also restraining the movement of the underlying mortar.

At smaller p/c ratios the PDA network was not properly developed at all examined locations. At some locations relatively small portions of PDA films were formed, but not enough to coalesce into a continuous structure. Figure 3.7-a illustrates an example case where PDA amount was insufficient to form a continuous surface or a PDA film. There were also places where PDA films were fully developed but there were not enough films to form a connected network (Figure 3.6-a). The confinement effectiveness improves with the continuity of the PDA film network. Example cases where PDA films provide partial and full encapsulation of cement are presented in Figure 3.7. The amount of discontinuous films decreased with increase in P/C. During extensive SEM examination of fracture surfaces, PDA films were never found detached from cement paste indicating that suitable bonding was achieved at interfaces which can be attributed to excellent adhesion properties of PDA.

3.3.3. AGGREGATE/BINDER INTERFACE

The aggregate/binder interface is considered the “weak link” in cement mortar because of two reasons: (1) The interface strength is typically smaller than the strength of the continuous cement paste, and (2) the porosity of the ITZ is up to four times higher than the porosity of the continuous paste due to “wall-effect” [10]. Incorporation of adhesive polymers has been found to improve the adhesion at such interfaces [6]. Due to its adhesion properties PDA is expected to increase the overall adhesion of binder and subsequently at aggregate/binder

interfaces. Those interfaces were examined under SEM and a representative micrograph showing a site of a dislodged sand particle is presented in Figure 3.8-a. A compound layer of PDA-cement occupying a large portion of the interface was noted. Several discontinuity sites were detected on this layer and are highlighted in the figure with arrows. Figure 3.8-b and 3.8-c show one of these discontinuity sites at a higher magnification. Clear boundaries differentiating the PDA and the underlying cement hydrates suggest that a local separation occurred within the PDA film as the aggregate was dislodged. This indicates a likely contribution of the PDA in enhancing the interface strength between aggregates and the surrounding composite matrix.

3.3.4. EFFECT OF PDA ON SPLITTING TENSILE STRENGTH

The effect of PDA on the tensile strength of mortar was evaluated by means of splitting tensile tests and the results are presented in Figure 3.9. The average strength increased approximately linearly with the p/c ratio. However, the standard deviations for both p/c=0.2% and p/c=0.5% were higher than plain mortar. This may happen due to difficulty of achieving a uniform distribution of polymer in large volumes of mortar at small p/c ratios which was also noted in other studies [5]. Mortar batches used in the casting of splitting tensile test specimens had a volume of about 12 times higher than that used for casting of compression test specimens. As the p/c ratio increases, so does the standard deviation of the measured strength. An enhanced tensile strength is a typical characteristic of PMMs compared with cement mortars, and is attributed to the

contribution of the polymer films. However these enhancements are typically observed at p/c ratios one order of magnitude higher than those used in the current study [11] as below a certain p/c ratio (typically 1-4%), an effective polymer network cannot be formed [3, 12]. The enhancement in tensile strength resulting from the incorporation of PDA was less pronounced than that in compressive strength. This can be reasonably explained by considering the contribution of porosity. In fact, it has been shown that even at small p/c ratios polymers can considerably reduce the porosity of mortar [12, 13, 9]. PDA may reduce the porosity similar to other polymers in PMM. Since the increase in compressive strength is typically larger than the increase in tensile strength due to porosity reduction [14] larger improvements in compressive strength can be expected.

3.4. EFFECT OF PDA ON RESTRAINED DRYING SHRINKAGE

The effect of PDA on the restrained drying shrinkage and the age at cracking of cement mortar was investigated using the ASTM C1581 ring test [15]. A summary of the test results are presented in Table 3.2. The average age at cracking for groups of control, p/c=0.2%, and p/c=0.5% was 13.5, 10, and 24.75 days, respectively. The reported maximum strain in the steel ring for each specimen is the maximum recorded strain among the three strain gages as specified in ASTM C1581 [15]. The average maximum steel ring strains for groups of control, p/c=0.2%, and p/c=0.5% were 80, 72, and 44 $\mu\varepsilon$, respectively. Cracks are defined as cracks that extended over at least one third of the height

of the specimen. Two cracks were found on each specimen in the groups of control and p/c=0.2% mortar. No cracks were found on the surface of the specimens with p/c=0.5%. The reported crack width is the average of three measurements at one fourth, one half, and three quarters of the crack length. The average crack width for groups of control and p/c=0.2% was 0.24 and 0.39 mm, respectively.

Plots of steel ring strain over time for different p/c ratios are shown in Figure 3.10. For each p/c ratio three curves are presented, two of which belong to a single specimen but different strain gages and one curve belongs to another specimen. Steel ring strain plots for all specimens of different groups are presented in Appendix 1. Specimen 1 from the group of p/c=0.2% and specimen 2 from the group of p/c=0.5% were discarded due to problems with data acquisition and were not considered in results analysis.

In case of control specimens, as illustrated in Figure 3.10 (a), different strain gages within one specimen, and different specimens exhibited similar shrinkage behavior. For the specimens of this group, shrinkage is controlled by water evaporation. As the internal water evaporates in time, the specimens shrink and the compressive strain in the steel rings increases. When the induced tensile stresses exceed the tensile strength of the cement mortar cracking occurs.

For the group of PDA-cement composites, the steel ring strain reflects the net shrinkage of the specimen which is the shrinkage caused by water evaporation minus the internal resistance to shrinkage caused by PDA films. In case of p/c=0.2%, as illustrated in Figure 3.10 (b), average maximum strain in the steel ring is smaller than the control group due to internal resistance to shrinkage caused by PDA films. This resistance originates from local confinement effect of PDA films and adhesion forces at the interfaces (see section 3.3.2). Another potential mechanism is the water retention effect of polymers. Literature shows that polymer films can entrap the internal water of fresh mortar reducing the evaporation rate [4]. Therefore the lower shrinkage can be attributed to a combined effect of reduced water loss and shrinkage resistance by PDA films. For specimens of this group (p/c = 0.2%), not only different specimens behaved differently but also different locations within one specimen exhibited different shrinkage behaviors. This inconsistency can be attributed to:

(1) Low PDA amount: as discussed in section 3.3.2 decreasing the p/c ratio increases the number of discontinuous PDA films. An example case obtained from 7-day compression test specimens is presented in Figure 3.11. Discontinuous PDA films act as defects and increase the heterogeneity of the matrix.

(2) The difficulty in distributing small polymer amounts in larger volumes of mortar.

Within one specimen, one strain gage experienced smaller net shrinkage (Figure 3.10 (b) specimen 2 SG2 – age 2-7 days) most likely because of being close to

locations where PDA films were concentrated whereas the other strain gage recorded progressive shrinkage in the same time period (Figure 3.10 (b) specimen 2 SG1). In this case, stress concentrations occur at locations of uneven shrinkage resulting in early cracking. As a result the age at cracking was 27% smaller than for the control specimens and with larger associated cracks (Table 3.2).

In case of p/c=0.5%, as illustrated in Figure 3.10 (c), the steel ring strain recorded by different strain gages within and between specimens were similar to each other and specimens exhibited a more consistent shrinkage behavior compared with p/c=0.2%. This improved consistency is attributed to formation of more uniformly distributed and continuous PDA films compared with the specimens having p/c = 0.2%. Between day 1 and day 6 of drying, the contribution of internal resistance to shrinkage by the PDA films, and possibly reduced water loss, reduced the net shrinkage of the specimens such that the compressive strain in the steel rings remained approximately constant instead of increasing as in the control and p/c = 0.2% specimens. At about day 7 of drying, shrinkage progresses most likely as a result of partial failure of the PDA network due to rupture of the less uniform and continuous portions of PDA film, and progressive separation at the interfaces subject to the internal stresses produced by shrinkage of the hydrated cement phases. The average maximum steel ring strain was reduced by 39% compared with specimens of p/c=0.2% due to higher contribution of PDA. From about day 10 of drying the PDA network and cement

hydrates co-resist the tensile stresses arising from drying shrinkage until cracking. As a result, the age at cracking of the PDA-cement mortar specimens with p/c=0.5% increased by 69% compared with the cement mortar counterparts. In addition, SEM analysis suggests that PDA films may contribute to resisting tensile stresses and offsetting crack formation and growth by bridging between defects and cracks. Figure 3.12 presents a SEM micrograph obtained from shrinkage specimens of p/c=0.5% illustrating potential crack-bridging effects. In fact, crack-bridging effects have been reported in previous studies on PMMs [2, 15], as illustrated in Figure 3.13 [7].

3.5. REFERENCES

[1] Lee H. Mussel-inspired surface chemistry for multifunctional coatings. Science 2007; 318(5849): 426-430.

[2] Sakai E, and Sugita J. Composite mechanism of polymer modified cement. Cement Concrete Res 1995; 25(1): 127-135.

[3] Saija LM. Waterproofing of Portland cement mortars with a specially designed polyacrylic latex. Cement Concrete Res 1995; 25(3): 503-509.

[4] Pascal S, Alliche A, and Pilvin P. Mechanical behaviour of polymer modified mortars. Mater Sci Eng A 2004; 380(1): 1-8.

[5] Jenni A, Holzer L, Zurbriggen R, and Herwegh M. Influence of polymers on microstructure and adhesive strength of cementitious tile adhesive mortars. Cement Concrete Res 2005; 35(1): 35-50.

[6] Afridi MUK, Ohama Y, Demura K, and Iqbal MZ. Development of polymer films by the coalescence of polymer particles in powdered and aqueous polymer-modified mortars. Cement Concrete Res 2003; 33(11): 1715-1721.

[7] Ohama Y. Handbook of polymer-modified concrete and mortars: properties and process technology. Koriyama (Japan): Noyes Publications 1995.

[8] Silva DA, Roman HR, and Gleize PJP. Evidences of chemical interaction between EVA and hydrating Portland cement. Cement Concrete Res 2002; 32(9): 1383-1390.

[9] Gao JM, Qian CX, Wang, B and Morino K. Experimental study on properties of polymer-modified cement mortars with silica fume. Cement Concrete Res 2002; 32(1): 41-45.

[10] Scrivener KL, Crumbie AK, and Laugesen P. The interfacial transition zone (ITZ) between cement paste and aggregate in concrete. Interface Sci 2004; 12(4): 411-421.

[11] Fowler DW. Polymers in concrete: a vision for the 21st century. Cement Concrete Comp 1999; 21(5): 449-452.

[12] Yang Z, Shi X, Creighton AT, and Peterson MM. Effect of styrene–butadiene rubber latex on the chloride permeability and microstructure of Portland cement mortar. Constr Build Mater 2009; 23(6): 2283-2290.

[13] Silva DA, John VM, Ribeiro JLD, and Roman HR. Pore size distribution of hydrated cement pastes modified with polymers. Cement Concrete Res 2001; 31(8): 1177-1184.

[14] Chen X, Wu S, and Zhou J. Influence of porosity on compressive and tensile strength of cement mortar. Constr Build Mater 2013; 40: 869-874.

[15] ASTM Standard C1581/C1581M 2009a. Standard test method for determining age at cracking and induced tensile stress characteristics of mortar and concrete under restrained shrinkage. ASTM International, West Conshohocken, PA, 2009, DOI: 10.1520/C1581_C1581M-09A, www.astm.org.

3.6. TABLES

Table 3.1 - Compression test results for all groups.

	After 7 days		After 28 days	
Group	Compressive strength [MPa]	Δ (%)	Compressive strength [MPa]	Δ (%)
Control	23.0 ± 3.1	-	35.5 ± 5.9	-
PDA1	25.3 ± 3.7	10.0	40.5 ± 5.6	14.1
PDA2	34.3 ± 2.0	49.1	43.6 ± 3.5	22.8
PDA5	39.2 ± 3.6	70.4	55.1 ± 4.8	55.2

Table 3.2 - Shrinkage test results for all specimens

				Average crack width [mm]		
Specimen	Age at cracking [day]	Maximum compressive strain [με]	Number of cracks	Crack 1	Crack 2	Average crack width [mm]
Control 1	14.5	65	2	0.13	0.22	0.18
Control 2	11.0	58	2	0.18	0.22	0.20
Control 3	14.5	78	2	0.45	0.24	0.35
PDA2 - 1	NA	NA	2	0.21	0.94	0.57
PDA2 - 2	10.0	65	2	0.26	0.27	0.26
PDA2 - 3	9.5	75	2	0.37	0.30	0.33
PDA5 - 1	24.0	38	0	-	-	-
PDA5 - 2	24.5	NA	0	-	-	-
PDA5 - 3	25.0	41	0	-	-	-

3.7. FIGURES

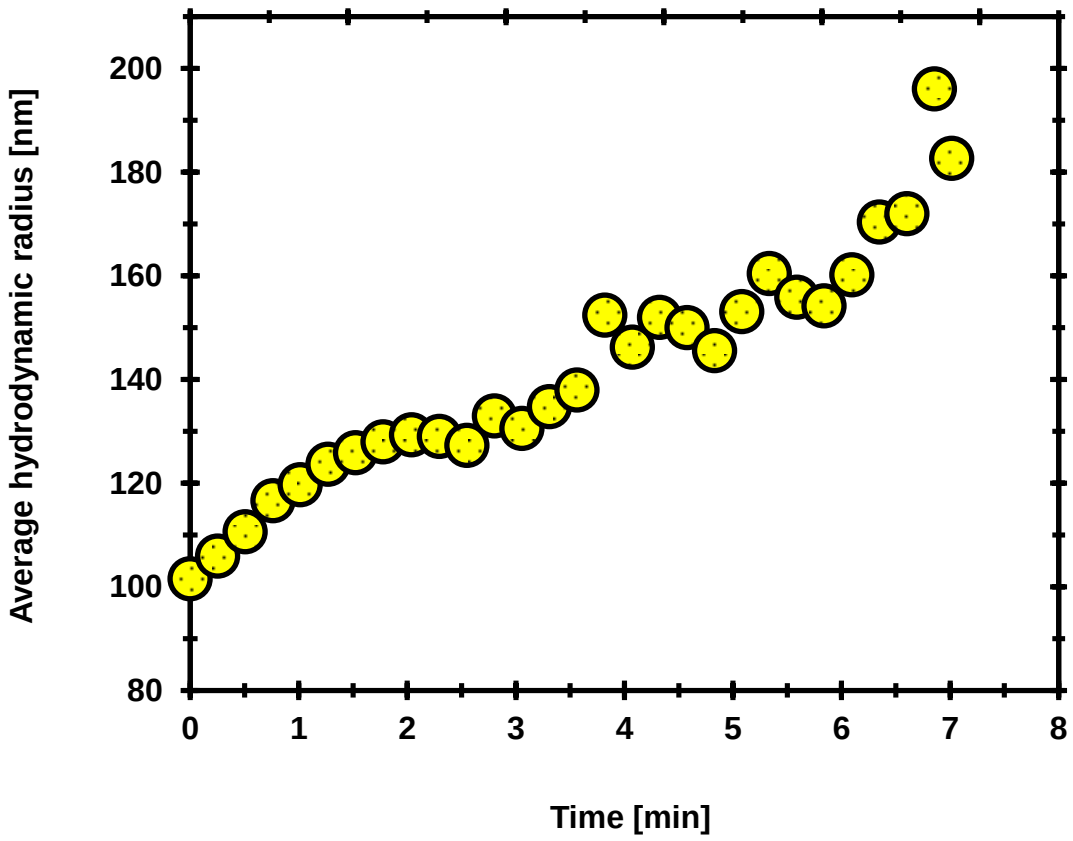

Figure 3.1 – PDA coil size profile – Coalescence of DA molecules into larger PDA particles in TRIS aqueous solution (polymerization)

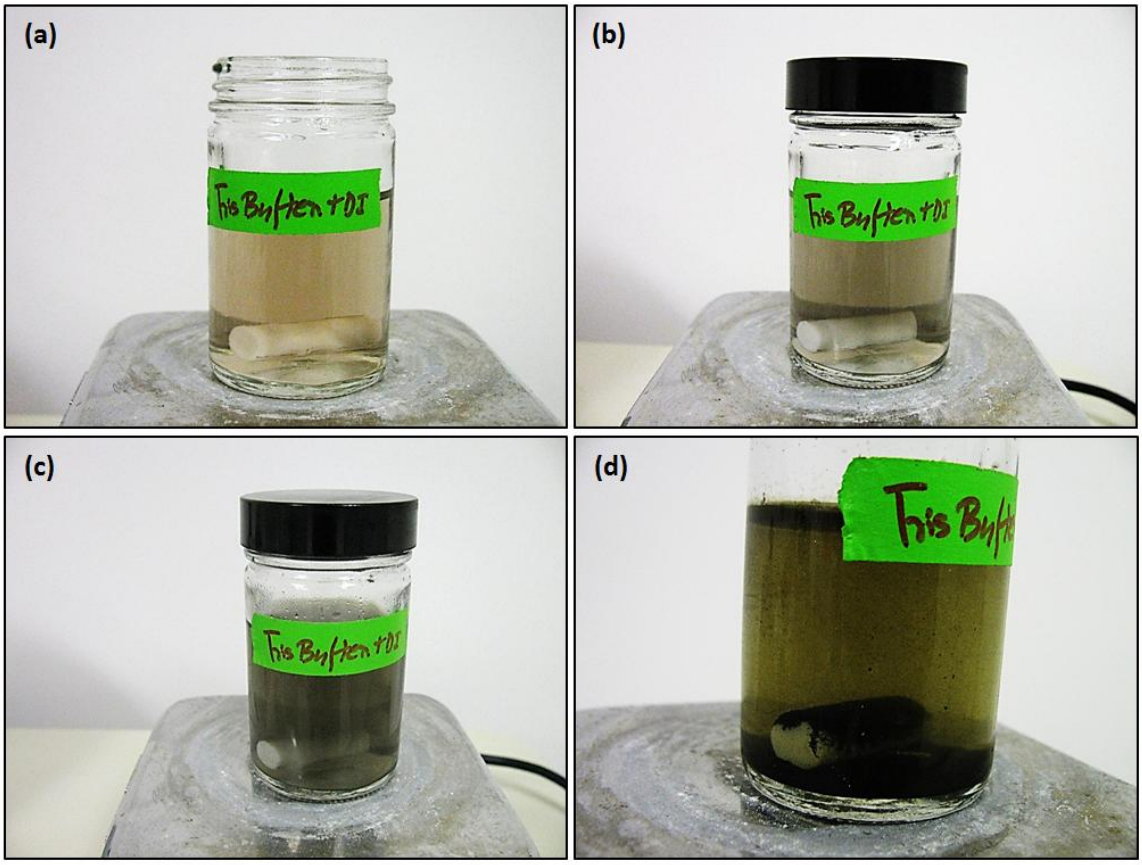

Figure 3.2 – DA polymerization progress in TRIS aqueous solution at different time intervals: (a) deposition initiation; (b) after 15 min; (c) after 3 hours; and (d) after 1 day of preparation.

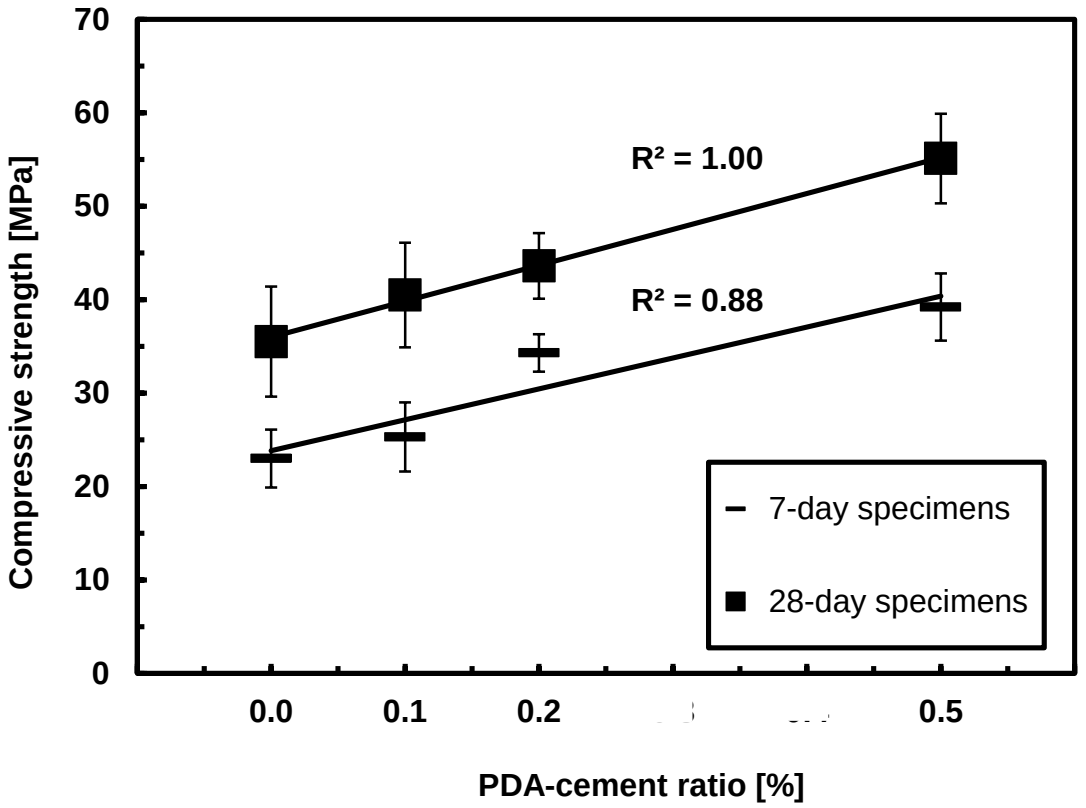

Figure 3.3 - Compressive strength of PDA-mortar at different p/c ratios

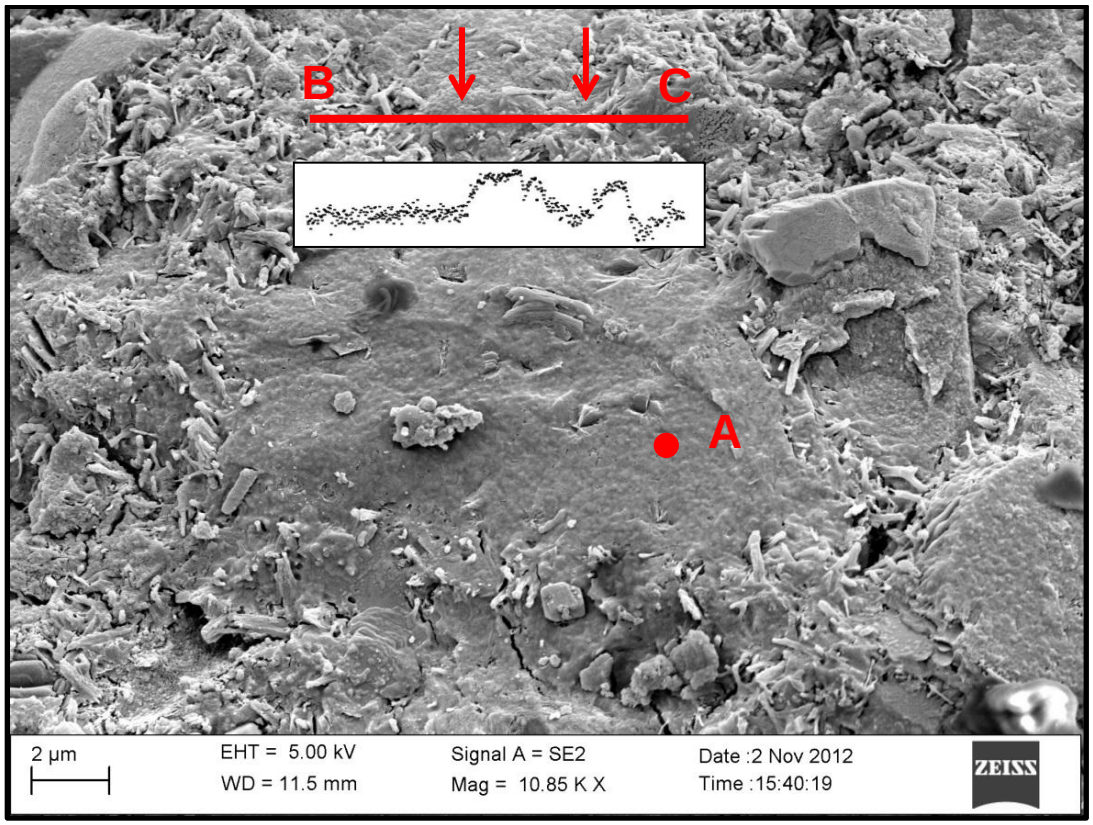

Figure 3.4 – SEM micrograph showing microstructure of PDA-cement matrix – Point A represents PDA film and line BC was selected such that it passed across cement paste and PDA film. The inset below line BC shows the variations in relative atomic concentration of carbon along the line

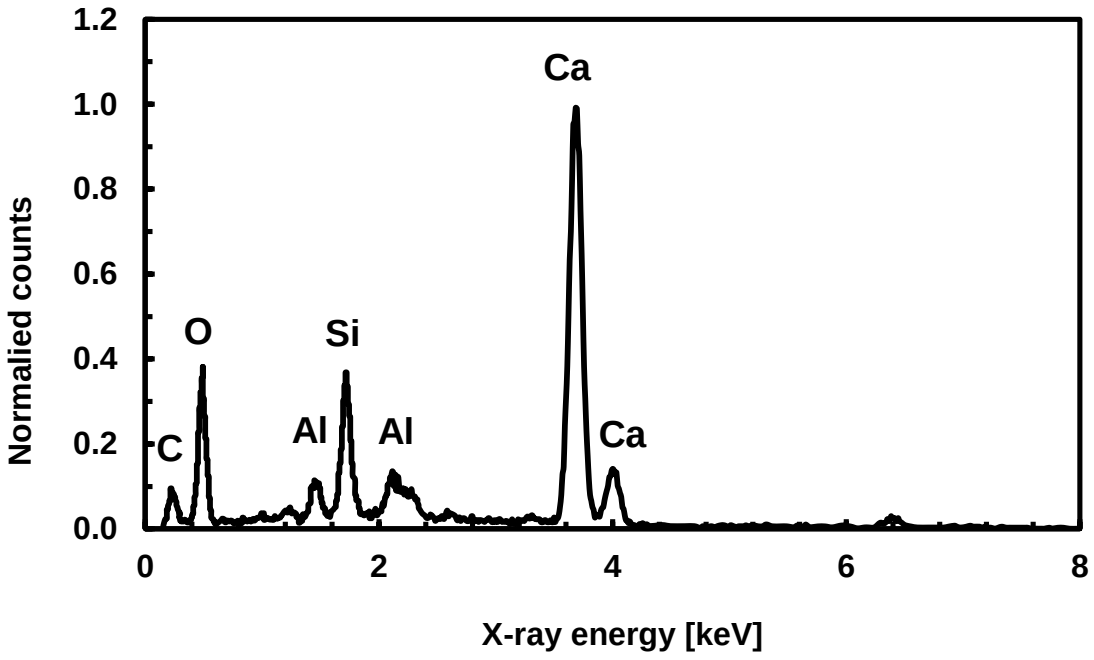

Figure 3.5 – X-ray spectrum of point A from Figure 3.4

(a)

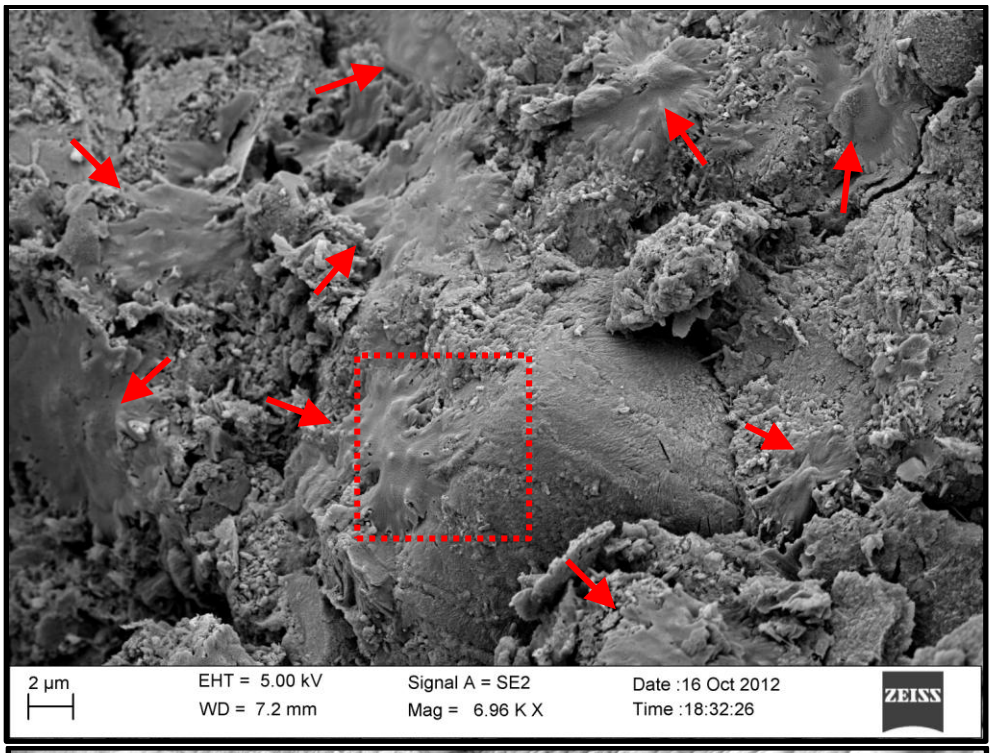

(b)

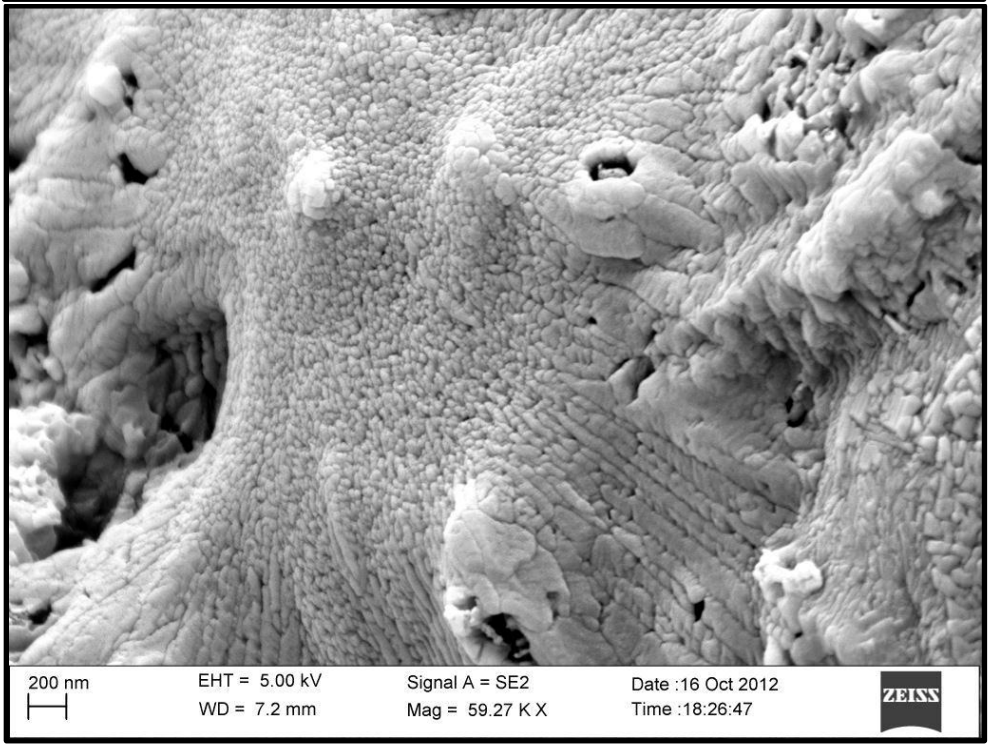

Figure 3.6 – Illustration of local PDA confinement mechanism: (a) PDA films partially encapsulating cement paste, (b) PDA film resisting stress. Arrows in (a) indicate PDA films

(a)

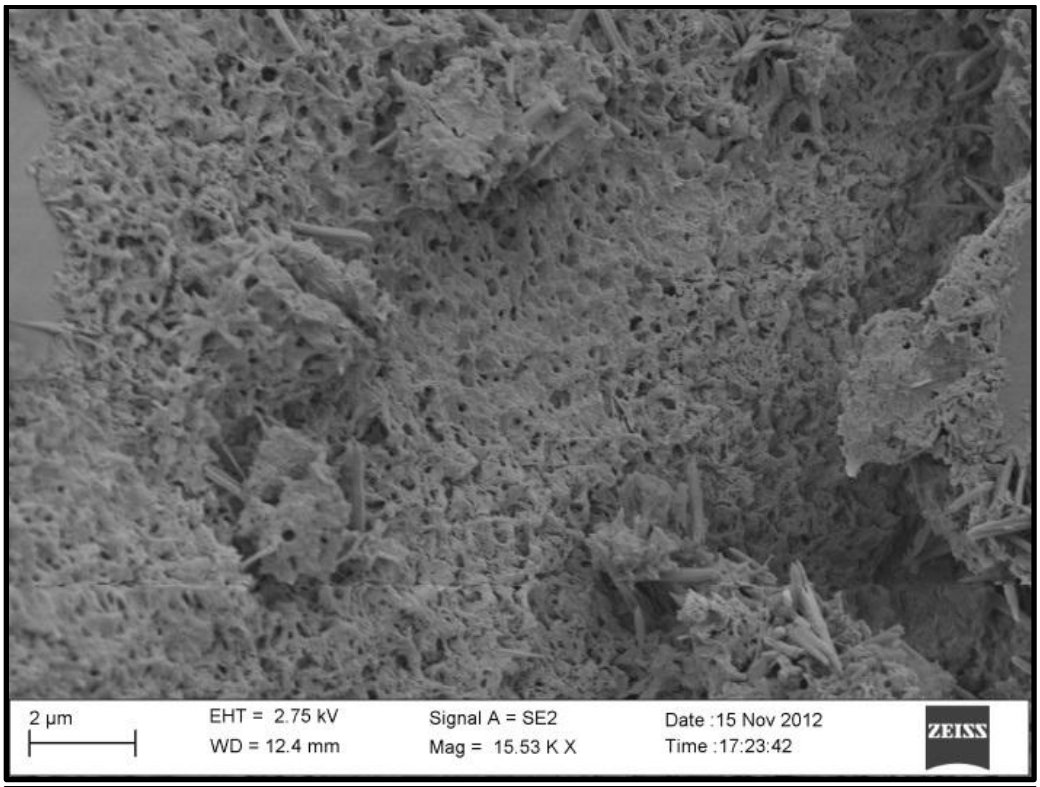

(b)

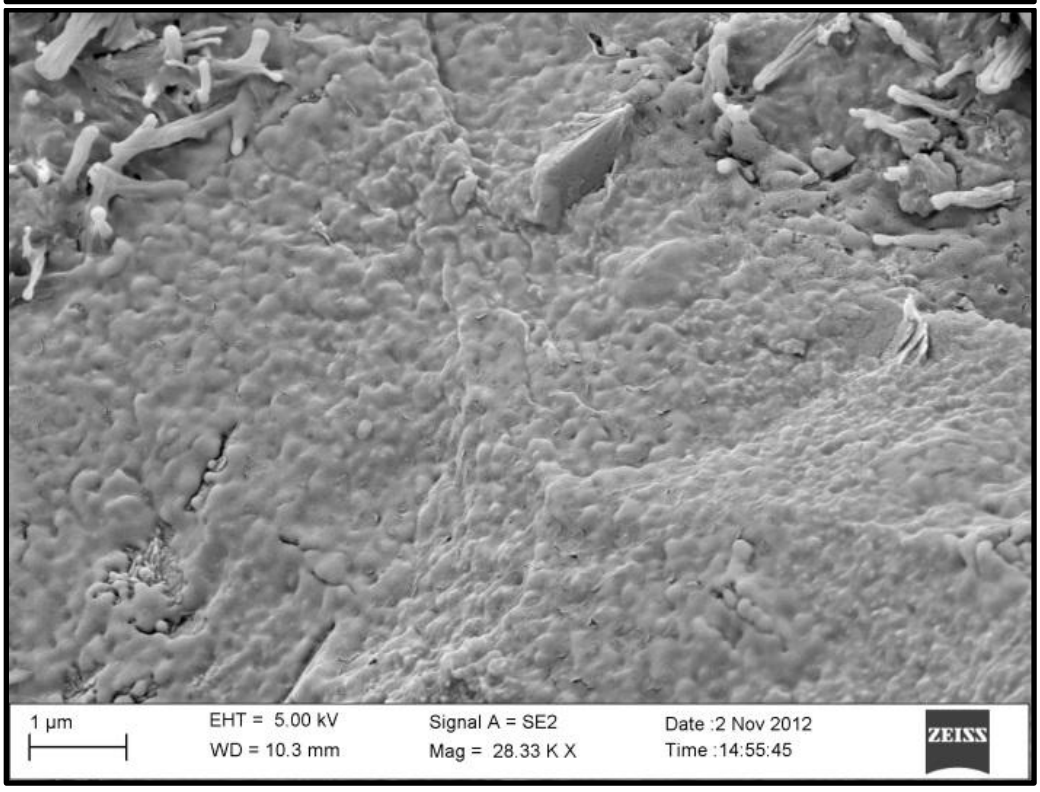

Figure 3.7 – Continuous and discontinuous PDA membranes – obtained from compressive strength samples of p/c=0.2% concentration: (a) poorly-formed discontinuous PDA membranes, (b) properly-formed continuous PDA membrane

(a)

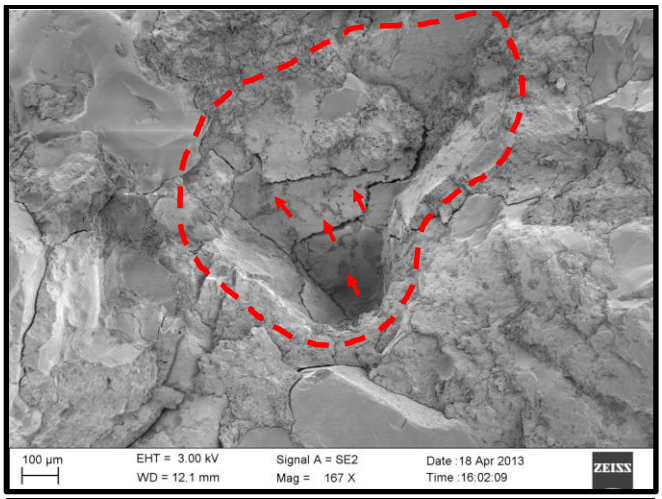

(b)

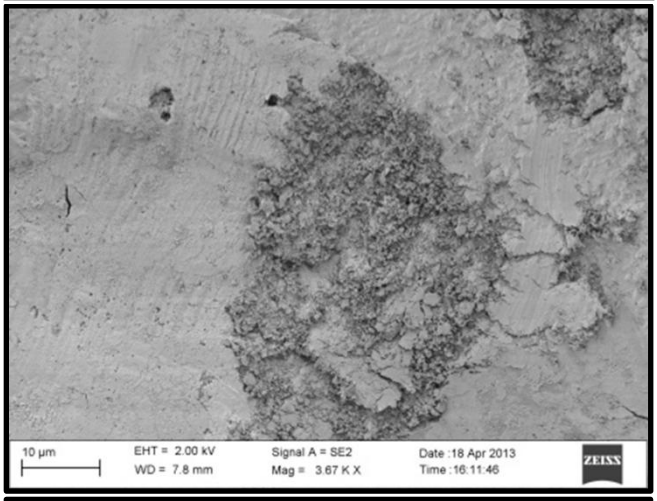

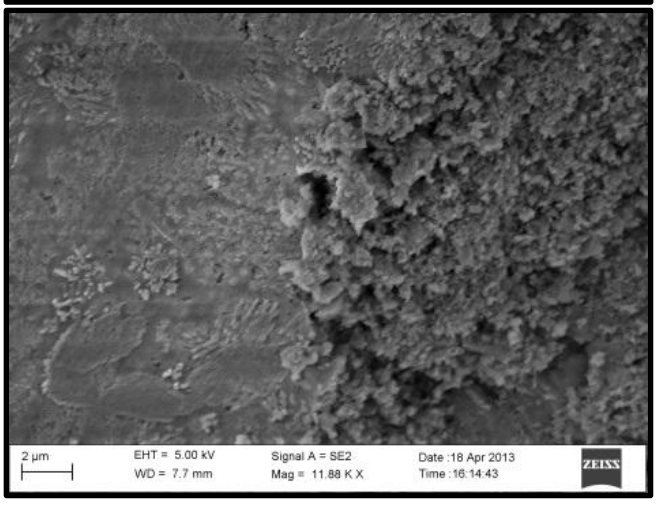

Figure 3.8 – (a) typical aggregate/binder interface in PDA-cement mortar, (b) detachment sites, (c) close-up of damage sites

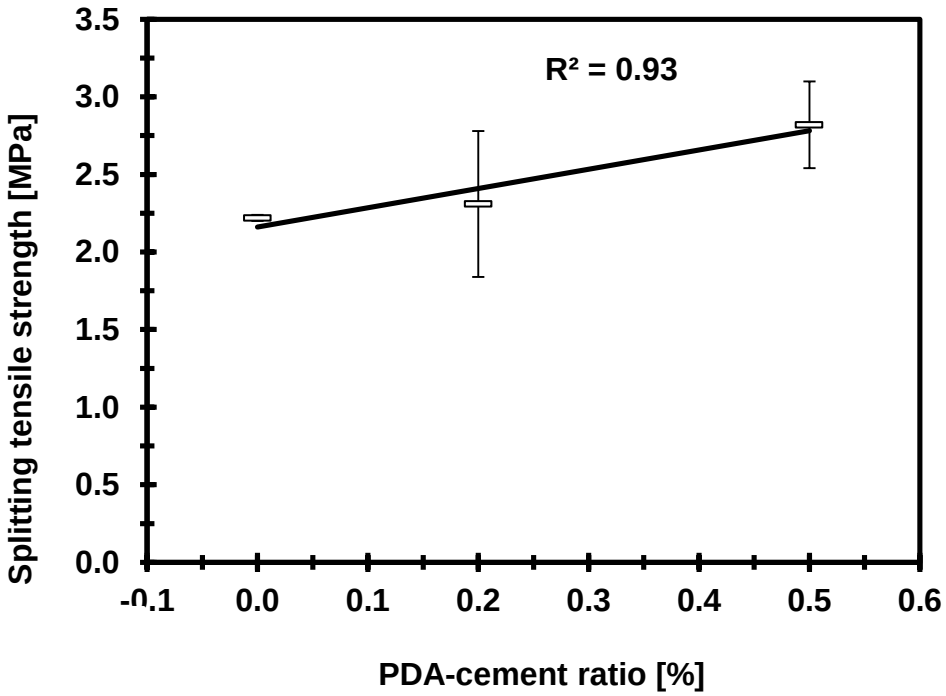

Figure 3.9 – Splitting tensile strength results

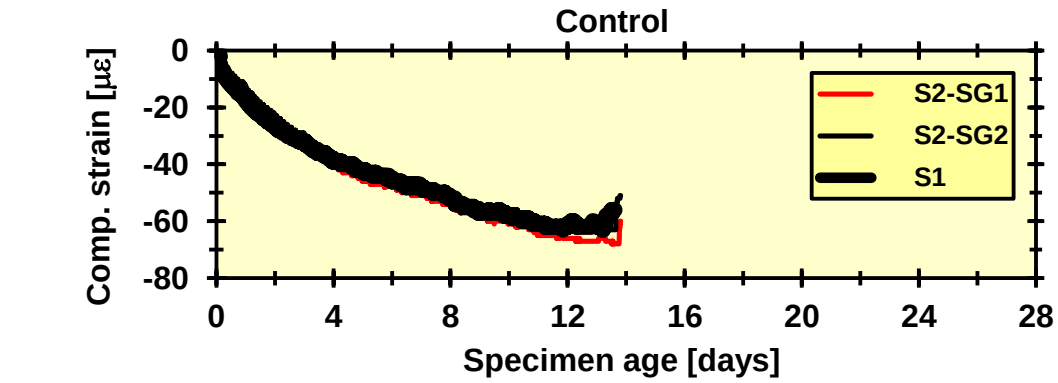

(a)

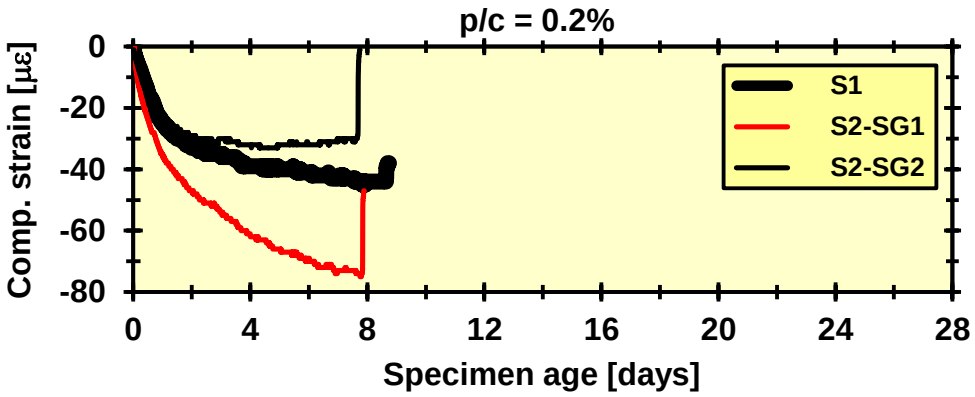

(b)

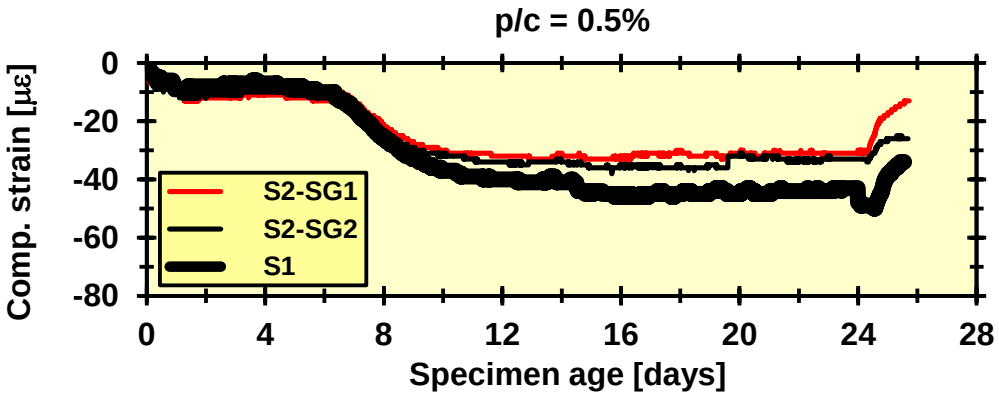

(c)

Figure 3.10 - Compressive strain in steel ring versus age of specimens: (a) Control specimens, (b) PDA-cement specimens – p/c=0.2%, and (c) PDA-cement specimens – p/c=0.5%

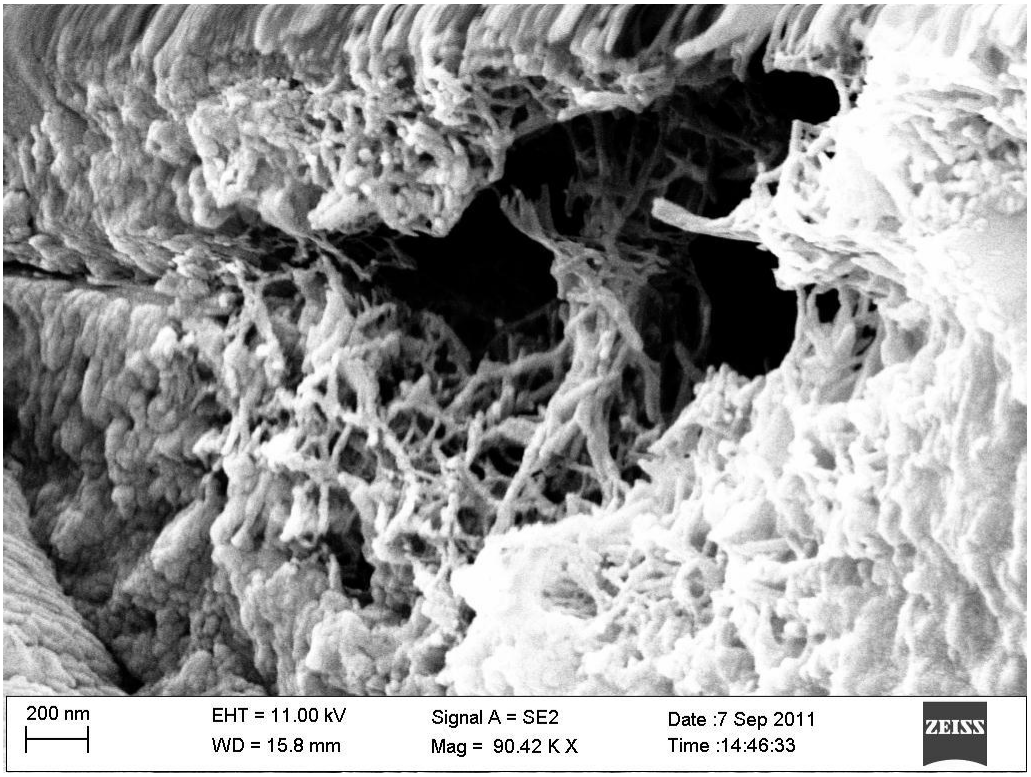

Figure 3.11 - Discontinuous PDA film in p/c=0.2%

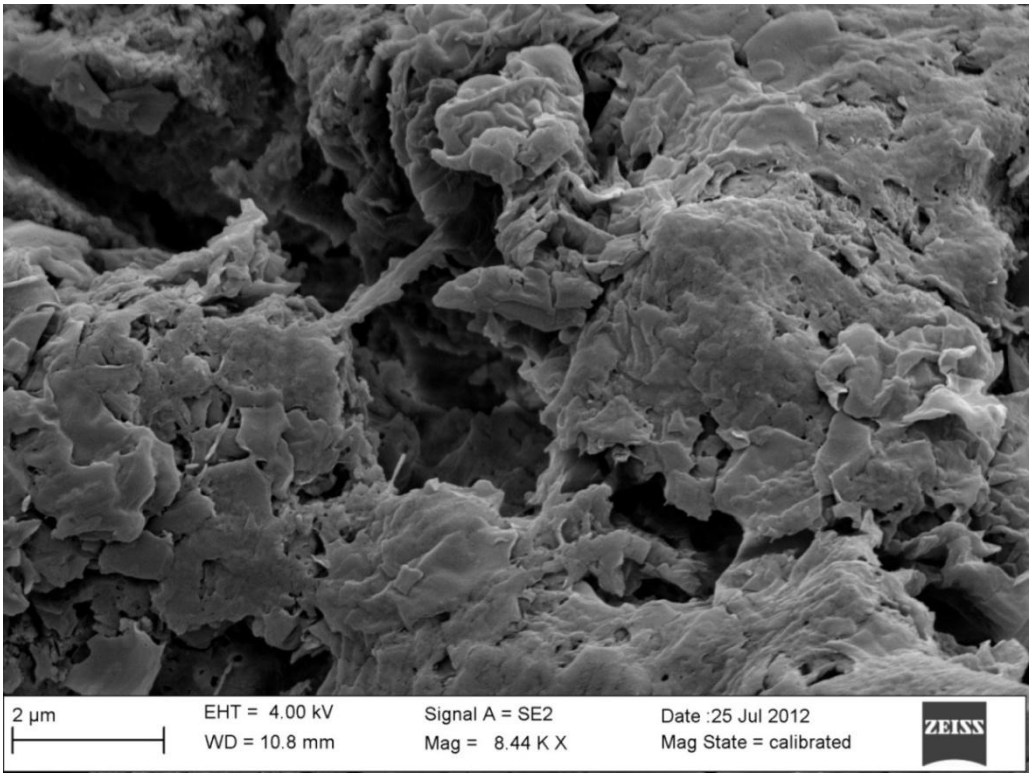

Figure 3.12 – SEM micrograph suggesting crack-bridging effect of PDA films

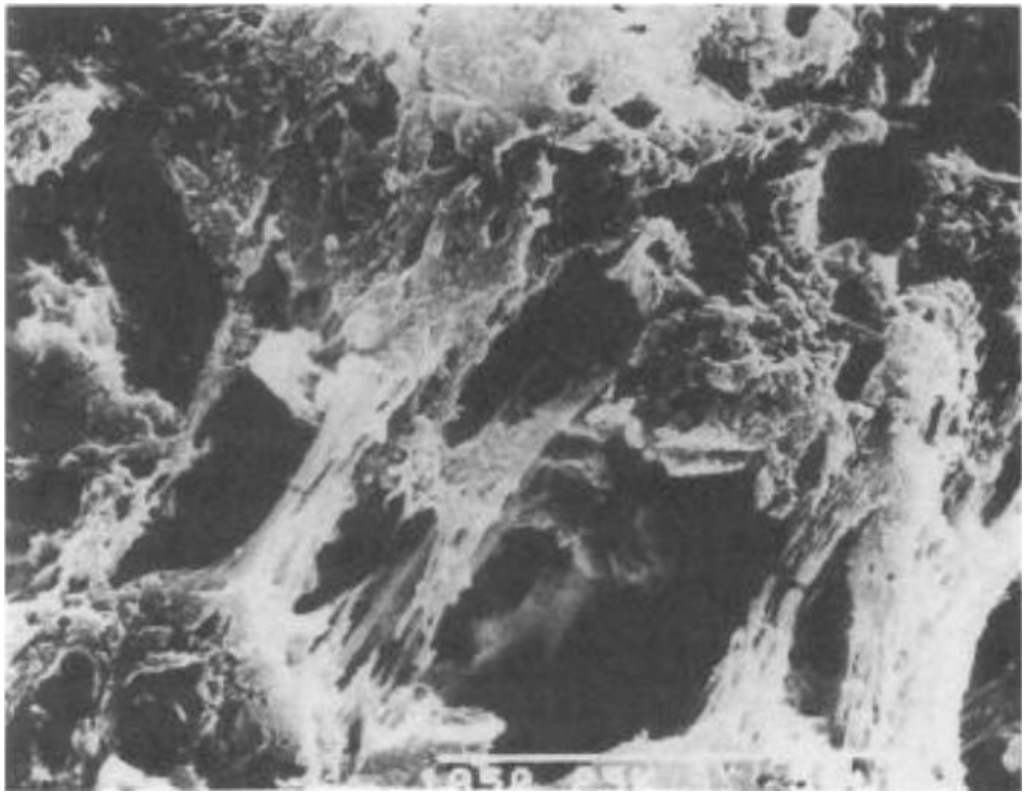

Figure 3.13 – Crack-bridging mechanism of polymer films in SBR-cement mortar [7]

CHAPTER 4

CONCLUSIONS AND RECOMMENDATIONS

In this study prototype PMM composites with mussel-inspired PDA at p/c ratios of 0.1-0.5% (one order of magnitude less than typical PMM) were produced and characterized based on compressive and splitting tensile strengths and restrained drying shrinkage. The morphology and microstructure of PDA-cement matrix was investigated using SEM/EDX analysis. Key findings can be summarized as:

- In 10 mM TRIS aqueous solution with pH=8.5 DA polymerizes forming adhesive layers of PDA.
- PDA incorporation improved the workability and reduced the setting time of fresh mixture.
- PDA appears in mortar matrix as continuous and dense structures that show good affinity with cement hydrates.
- In microstructure of PDA-cement mortar, PDA films participate to form a network that spreads throughout the composite matrix interpenetrating the cement hydrates. PDA films extend over mortar constituents restraining deformation of cement hydrates under stress creating a physical confinement for cement paste cells at a local level.
- The effectiveness of PDA incorporation depends on formation of continuous PDA films that are uniformly distributed throughout the composite. Increase in p/c increases the number of continuous PDA films and improves the homogeneity of the mixture.
- SEM analysis revealed presence of PDA at aggregate/binder interfaces. Damage marks at these interfaces suggest PDA enhanced interfacial

bond was achieved.

- Incorporation of PDA at p/c=0.5% increased the 7- and 28-day compressive strength of cement mortar by 70% and 55%, respectively. The same polymer content increased the splitting tensile strength by 27%.
- PDA at p/c=0.5% reduced the restrained drying shrinkage of cement mortar by 41% due to internal resistance to shrinkage caused by PDA films and the possible contribution of water-retention effect. The age at cracking was increased by 69% and no visible cracks were found on the surface of the specimens which can be attributed to PDA resistance to shrinkage through local confinement and interfacial adhesion forces. SEM analysis of fracture surface suggests the enhancement in age at cracking can be partially attributed to crack-bridging effect of PDA films.

Further studies should be conducted to investigate the effect of PDA on durability characteristics and in particular the permeability of PDA-cement mortar. Adhesion strength of PDA-cement mortar to different substrates at different p/c ratios and under different curing methods should be measured as an important property for all repair materials. Tests should be designed and conducted to evaluate the PDA resistance against different aggressive agents such acids, slats, oxygen, chloride and sulphate ions, and high temperatures. Creep characteristics of PDA-cement mortar should be studied under different environmental conditions.

CITED REFERENCES

ACI Committee 503. Guide for the selection of polymer adhesives with concrete. Farmington Hills, MI: American Concrete Institute 2003.

ACI Committee 548. Report on polymer-modified concrete. Farmington Hills, MI: American Concrete Institute 2009.

Afridi MUK, Ohama Y, Demura K, and Iqbal MZ. Development of polymer films by the coalescence of polymer particles in powdered and aqueous polymer-modified mortars. Cement Concrete Res 2003; 33(11): 1715-1721.

Afridi MUK, Ohama Y, Zafar Iqbal M, and Demura K. Water retention and adhesion of powdered and aqueous polymer-modified mortars." Cement Concrete Comp 1995; 17(2): 113-118.

Aggarwal LK, Thapliyal PC, and Karade SR. Properties of polymer-modified mortars using epoxy and acrylic emulsions. Constr Build Mater 2007; 21(2): 379-383.

Al-Zahrani MM, Al-Dulaijan SU, Ibrahim M, Saricimen H, and Sharif FM. Effect of waterproofing coatings on steel reinforcement corrosion and physical properties of concrete. Cement Concrete Comp 2002; 24(1): 127-137.

Al-Zahrani MM, Maslehuddin M, Al-Dulaijan SU, and Ibrahim M. Mechanical properties and durability characteristics of polymer-and cement-based repair materials. Cement Concrete Comp 2003; 25(4): 527-537.

Allen RTL, Edwards SC, and Shaw DN. Repair of concrete structures. Taylor & Francis 1992.

ASTM Standard C109/C109M 2013. Standard test method for compressive strength of hydraulic cement mortars (Using 2-in. or [50-mm] cube specimens). ASTM International, West Conshohocken, PA, 2013, DOI: 10.1520/C0109_C0109M, www.astm.org.

ASTM Standard C1581/C1581M 2009a. Standard test method for determining age at cracking and induced tensile stress characteristics of mortar and concrete under restrained shrinkage. ASTM International, West Conshohocken, PA, 2009, DOI: 10.1520/C1581_C1581M-09A, www.astm.org.

ASTM Standard C305 2013. Standard practice for mechanical mixing of hydraulic cement pastes and mortars of plastic consistency. ASTM International, West Conshohocken, PA, 2013, DOI: 10.1520/C0305, www.astm.org.

ASTM Standard C496/C496M 2011. Standard test method for splitting tensile strength of cylindrical concrete specimens. ASTM International, West Conshohocken, PA, 2011, DOI: 10.1520/C0496_C0496M-11, www.astm.org.

ASTM Standard C778 2013. Standard specification for standard sand. ASTM International, West Conshohocken, PA, 2013, DOI: 10.1520/C0778, www.astm.org.

Barluenga G, and Hernández-Olivares F. SBR latex modified mortar rheology and mechanical behaviour. Cement Concrete Res 2004; 34(3): 527-535.

Brandt AM. Cement-based composited: materials, mechanical properties and performance. New York: Taylor & Francis, 2009.

Chen X, Wu S, and Zhou J. Influence of porosity on compressive and tensile strength of cement mortar. Constr Build Mater 2013; 40: 869-874.

Chung DDL. Use of polymers for cement-based structural materials. J Mater Sci 2004; 39(9): 2973-2978.

Dreyer DR, Miller DJ, Freeman BD, Paul DR, Bielawski CW. Elucidating the structure of poly(dopamine). Langmuir 2012; 28(15): 6428-6435.

Filho RDT, Ghavami K, Sanjuán MA, and England GL. Free, restrained and drying shrinkage of cement mortar composites reinforced with vegetable fibres. Cement and Concrete Comp 2005; 27(5): 537-546.

Fowler DW. Polymers in concrete: a vision for the 21st century. Cement Concrete Comp 1999; 21(5): 449-452.

Fu X, and Chung DDL. Effect of polymer admixtures to cement on the bond strength and electrical contact resistivity between steel fiber and cement. Cement Concrete Res 1996; 26(2): 189-194.

Gao JM, Qian CX, Wang, B and Morino K. Experimental study on properties of polymer-modified cement mortars with silica fume. Cement Concrete Res 2002; 32(1): 41-45.

Han G, Zhang S, Li X, Widjojo N, and Chung TS. Thin film composite forward osmosis membranes based on polydopamine modified polysulfone substrates with enhancements in both water flux and salt rejection. Chem Eng Sci 2012; 80: 219-231.

Hossain AB, and Weiss J. Assessing residual stress development and stress relaxation in restrained concrete ring specimens. Cement and Concrete Comp 2004; 26(5): 531-540.

Jenni A, Holzer L, Zurbriggen R, and Herwegh M. Influence of polymers on microstructure and adhesive strength of cementitious tile adhesive mortars. Cement Concrete Res 2005; 35(1): 35-50.

Jenni A, Zurbriggen R, Holzer L, and Herwegh M. Changes in microstructures and physical properties of polymer-modified mortars during wet storage. Cement Concrete Res 2006; 36(1): 79-90.

Kardon JB. Polymer-modified concrete: review. J Mater Civil Eng 1997; 9(2): 85-92.

Knapen E, and Van Gemert D. Cement hydration and microstructure formation in the presence of water-soluble polymers. Cement Concrete Res 2009; 39(1): 6-13.

Lee H. Mussel-inspired surface chemistry for multifunctional coatings. Science 2007; 318(5849): 426-430.

Li B, Liu W, Jiang Z, Dong X, Wang B, Zhong Y. Ultrathin and stable layer of dense composite membrane enabled by poly(dopamine). Langmuir 2009; 25(13): 7368-7374.

Liao Y, Cao B, Wang WC, Zhang L, Wu D, Jin R. A facile method for preparing highly conductive and reflective surface-silvered polyimide films. Appl Surf Sci 2009; 255(19): 8207-8212.

McLaskey GC, Glaser SD, and Grosse CU. Integrating broad-band high-fidelity acoustic emission sensors and array processing to study drying shrinkage cracking in concrete. In The 14th International Symposium on: Smart Structures and Materials & Nondestructive Evaluation and Health Monitoring, pp. 65290C-65290C. International Society for Optics and Photonics, 2007.

Nepomuceno AN, and Andrade C. Steel protection capacity of polymeric based cement mortars against chloride and carbonation attacks studied using electrochemical polarization resistance. Cement Concrete Comp 2006; 28(8): 716-721.

Ohama Y. Handbook of polymer-modified concrete and mortars: properties and process technology. Koriyama (Japan): Noyes Publications 1995.

Ohama Y. Study on properties and mix proportioning of polymer modified mortars for buildings. Report of the Building Research Institute 1973; 65: 170.
Pascal S, Alliche A, and Pilvin P. Mechanical behaviour of polymer modified mortars. Mater Sci Eng A 2004; 380(1): 1-8.

Pease B, Shah H, and Weiss J. Shrinkage behavior and residual stress development in mortar containing shrinkage reducing admixtures (SRAs). ACI Special Publication 227 (2005).

Reis JML. Mechanical characterization of polymer mortars exposed to degradation solutions. Constr Build Mater 2009; 23(11): 3328-3331.

Rossignolo JA. Interfacial interactions in concretes with silica fume and SBR latex. J Constr Build Mater 2009; 23(2): 817-821.

Saija LM. Waterproofing of Portland cement mortars with a specially designed polyacrylic latex. Cement Concrete Res 1995; 25(3): 503-509.

Sakai E, and Sugita J. Composite mechanism of polymer modified cement. Cement Concrete Res 1995; 25(1): 127-135.

Salomone JC (Ed). Concise polymeric materials encyclopedia. CRC press 1999; 1: 278-281.

Scrivener KL, Crumbie AK, and Laugesen P. The interfacial transition zone (ITZ) between cement paste and aggregate in concrete. Interface Sci 2004; 12(4): 411-421.

Shah HR, and Weiss J. Quantifying shrinkage cracking in fiber reinforced concrete using the ring test. Mater Struct 2006; 39(9): 887-899

Silva DA, John VM, Ribeiro JLD, and Roman HR. Pore size distribution of hydrated cement pastes modified with polymers. Cement Concrete Res 2001; 31(8): 1177-1184.

Silva DA, Roman HR, and Gleize PJP. Evidences of chemical interaction between EVA and hydrating Portland cement. Cement Concrete Res 2002; 32(9): 1383-1390.

Van Gemert D, Czarnecki L, Maultzsch M, Schorn H, Beeldens A, Łukowski P, and Knapen E. Cement concrete and concrete–polymer composites: Two merging worlds: A report from 11th ICPIC Congress in Berlin, 2004. Cement Concrete Comp 2005; 27(9): 926-933.

Wang R, Li XG, and Wang PM. Influence of polymer on cement hydration in SBR-modified cement pastes. Cement Concrete Res 2006; 36(9): 1744-1751.

Yang Z, Shi X, Creighton AT, and Peterson MM. Effect of styrene–butadiene rubber latex on the chloride permeability and microstructure of Portland cement mortar. Constr Build Mater 2009; 23(6): 2283-2290.

APPENDIX A

STEEL RING STRAIN PLOTS FOR DIFFERENT GROUPS

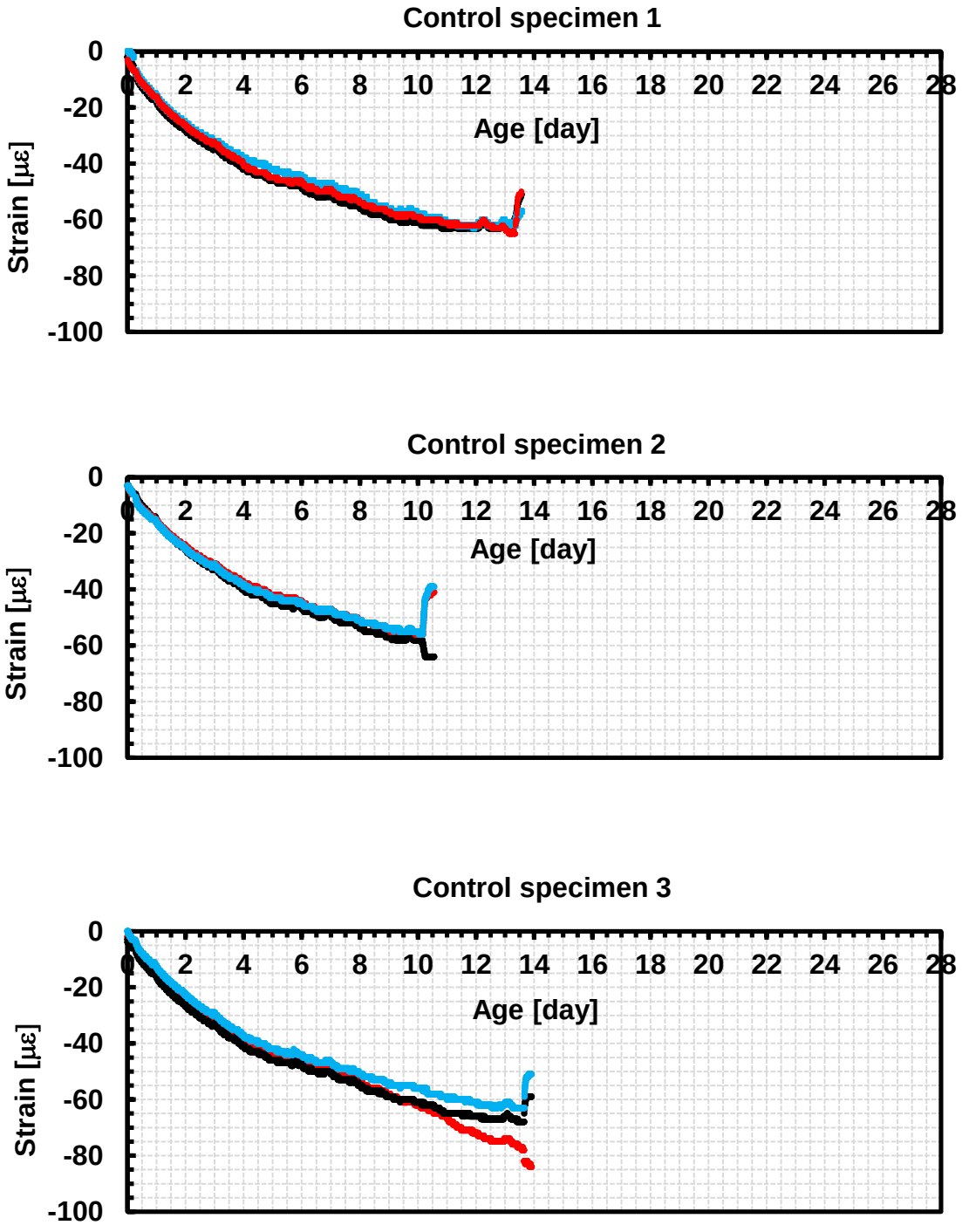

Figure A.1 – Steel ring strain for all control specimens

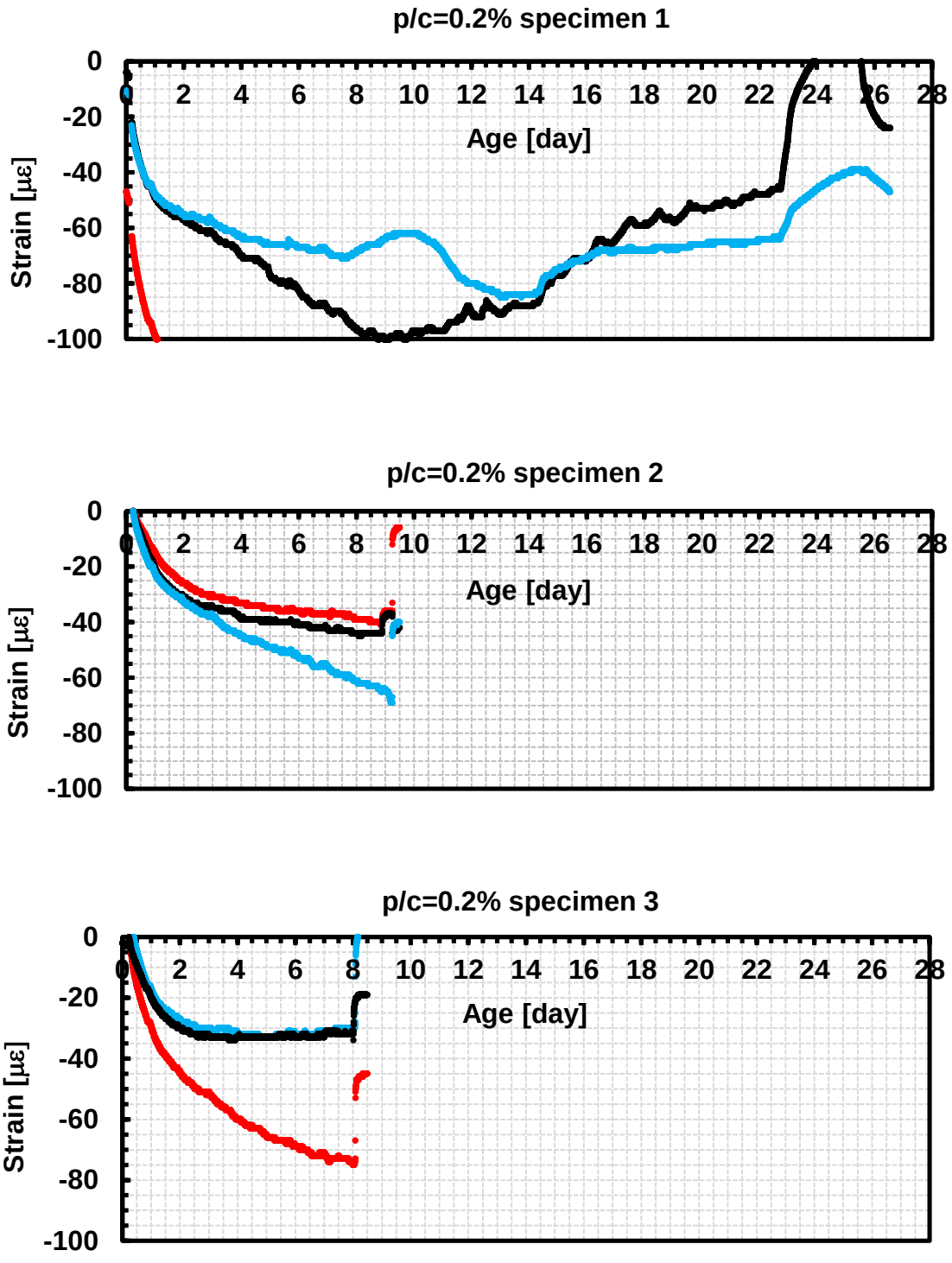

Figure A.2 – Steel ring strain for all specimens of p/c=0.2%

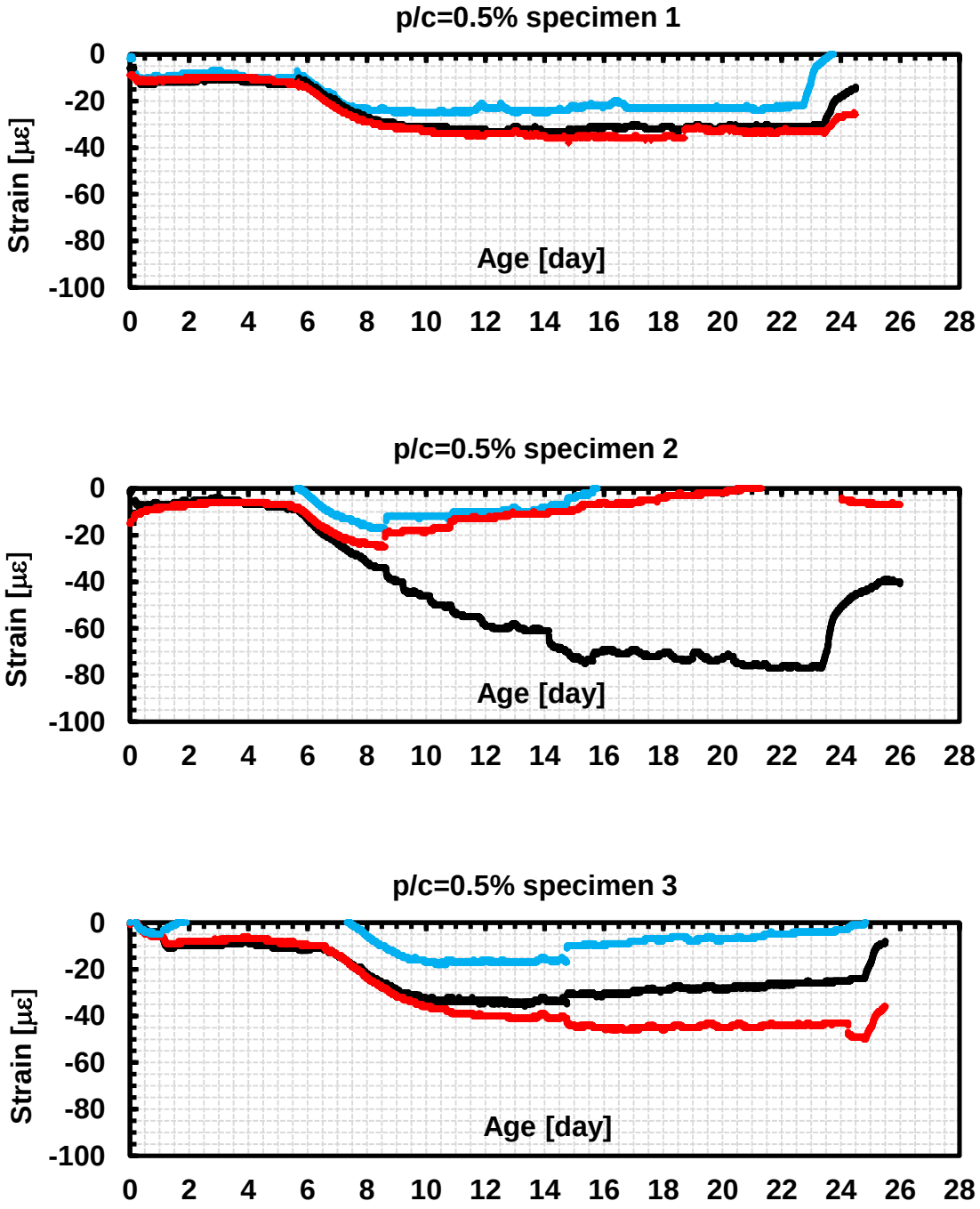

Figure A.3 – Steel ring strain for all specimens of p/c=0.5%

APPENDIX B

COMPARISON OF MOLECULAR STRUCTURE OF DA AND COMMON POLYMERS USED IN PRODUCTION OF CONVENTIONAL PMMS

The presence of hydroxyl (OH) groups on the monomer, DA, and polymer, PDA, of dopamine (Figure 1a and b) offers likely deprotonation when added to water, leaving negatively charged reactive O– sites to electrostatically interact with positively charged cations and the crystal structure of cement mortar. The negatively charged O– groups remain available for electrostatic interaction during the polymerization of dopamine. The presence of two charged sites per monomer of dopamine makes this polymer a strongly interacting cement mortar additive that binds the cement matrix via stronger electrostatic interaction compared to interfacial adhesion, where the latter mechanism is typical for most polymers used in PMMs.

Commonly used polymers, e.g., polypropylene or cellulose ether, either possess less number of charged functional groups (e.g., O–) per monomer or do not possess any such reactive groups at all. Thus, these polymers mostly interact with the cement mortar via a weaker interfacial attachment compared to the electrostatic interaction that likely occurs with dopamine. Figure 2 presents the monomer structures as well as the typical polymerization scheme of polypropylene and cellulose ether, demonstrating the absence of charged functional groups.

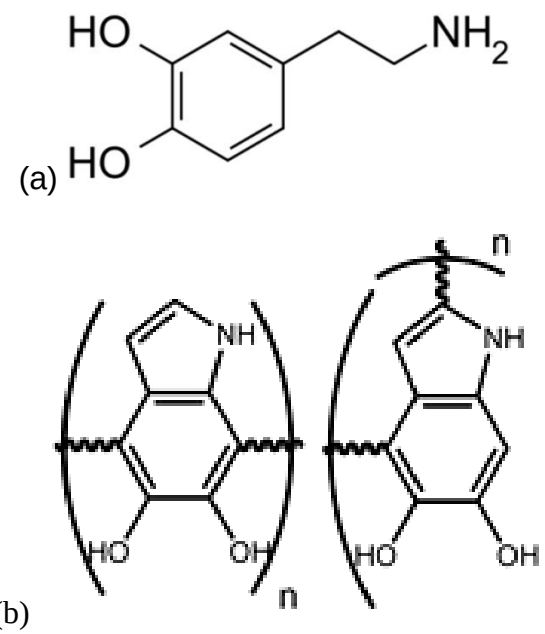

Figure B.1 - Molecular structure of (a) DA, (b) PDA

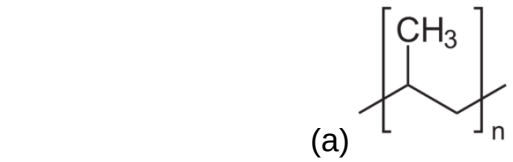

(a)

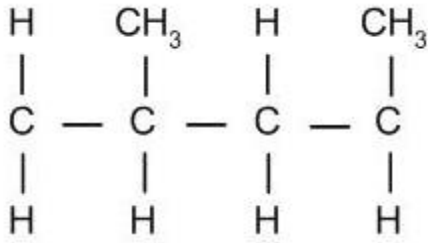

(b)

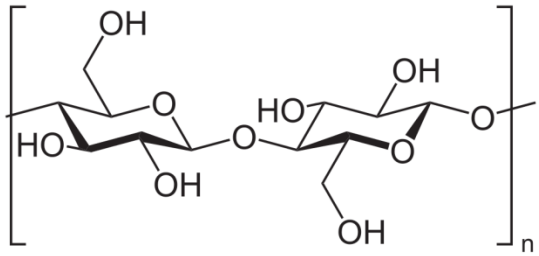

(c)

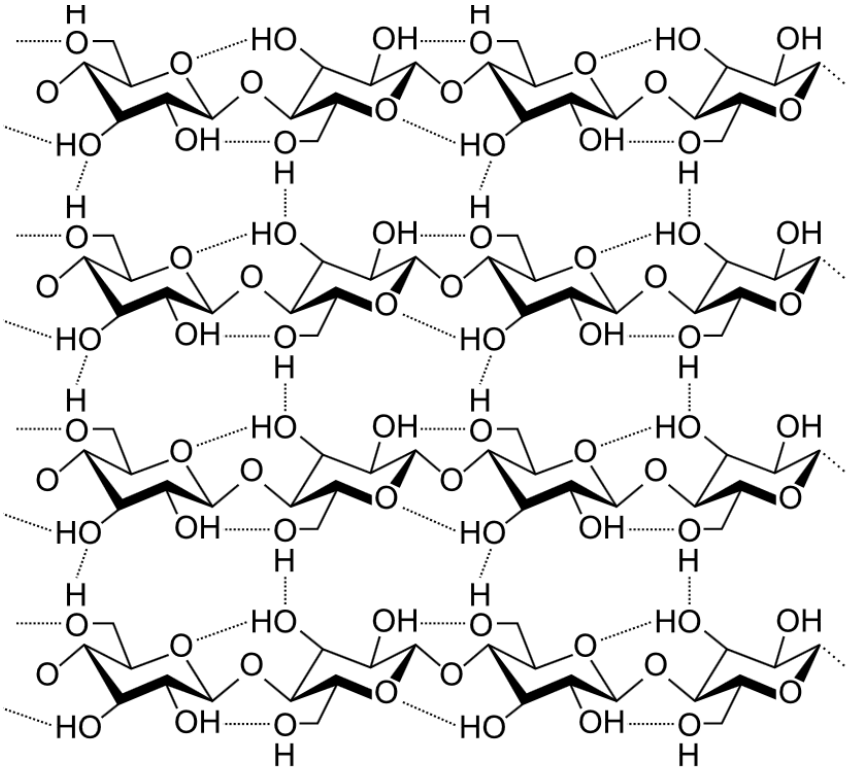

(d)

Figure B.2 - Molecular structure of (a) propylene, (b) polypropylene, (c) cellulose ether, and (d) polymer of cellulose ether